

Boolean Delay Equations: A Simple Way of Looking at Complex Systems

Michael Ghil,^{1,2,3} Ilya Zaliapin,^{3,4} and Barbara Coluzzi⁵

¹ *Département Terre-Atmosphère-Océan and Laboratoire de Météorologie Dynamique (CNRS and IPSL), Ecole Normale Supérieure, 24 rue Lhomond, F-75231 Paris Cedex 05, FRANCE, E-mail: ghil@lmd.ens.fr, Phone: 33-(0)1-4432-2244, Fax: 33-(0)1-4336-8392, corresponding author.*

² *Department of Atmospheric and Oceanic Sciences, University of California, Los Angeles, CA 90095-1565, USA.*

³ *Institute of Geophysics and Planetary Physics, University of California, Los Angeles, CA 90095-1567, USA.*

⁴ *Department of Mathematics and Statistics, University of Nevada, Reno, NV 89557, USA. E-mail: zal@unr.edu*

⁵ *Environmental Research and Teaching Institute, Ecole Normale Supérieure, F-75231 Paris Cedex 05, FRANCE. E-mail: coluzzi@lmd.ens.fr*

Abstract. Boolean Delay Equations (BDEs) are a novel type of semi-discrete dynamical models with Boolean-valued variables that evolve in continuous time. Systems of BDEs can be classified into *conservative* or *dissipative*, in a manner that parallels the classification of ordinary or partial differential equations. Solutions to certain conservative BDEs exhibit growth of complexity in time. They represent therewith metaphors for biological evolution or human history. Dissipative BDEs are structurally stable and exhibit multiple equilibria and limit cycles, as well as more complex, fractal solution sets, such as Devil’s staircases and “fractal sunbursts.” All known solutions of dissipative BDEs have stationary variance. BDE systems of this type, both free and forced, have been used as highly idealized models of climate change on interannual, interdecadal and paleoclimatic time scales. BDEs are also being used as flexible, highly efficient models of colliding cascades in earthquake modeling and prediction, as well as in genetics. Some of the climatic and solid-earth applications are illustrated; the former have used small systems of BDEs, while the latter have used large networks of BDEs. We introduce BDEs with an infinite number of variables distributed in space (“partial BDEs”) and discuss connections with other types of dynamical systems, including cellular automata and Boolean networks. This research-and-review paper concludes with a set of open questions.

PACS: 02.30.Ks (Delay and functional equations); 05.45.Df (Fractals); 91.30.Dk (Seismicity); 92.70.Pq (Earth system modeling)

Keywords: Discrete dynamical systems, Earthquakes, El-Niño/Southern-Oscillation, Increasing complexity, Phase diagram, Prediction.

1 Introduction

BDEs are a novel modeling framework especially tailored for the mathematical formulation of conceptual models of systems that exhibit threshold behavior, multiple feedbacks

and distinct time delays [1, 2, 3, 4]. BDEs are intended as a heuristic first step on the way to understanding problems too complex to model using systems of partial differential equations at the present time. One hopes, of course, to be able to eventually write down and solve the exact equations that govern the most intricate phenomena. Still, in the geosciences as well as in the life sciences and elsewhere in the natural sciences, much of the preliminary discourse is often conceptual.

BDEs offer a formal mathematical language that may help bridge the gap between qualitative and quantitative reasoning. Besides, they are fun to play with and produce beautiful fractals [5], by simple, purely deterministic rules.

In a hierarchical modeling framework, simple conceptual models are typically used to present hypotheses and capture isolated mechanisms, while more detailed models try to simulate the phenomena more realistically and test for the presence and effect of the suggested mechanisms by direct confrontation with observations [6]. BDE modeling may be the simplest representation of the relevant physical concepts. At the same time new results obtained with a BDE model often capture phenomena not yet found by using conventional tools [7, 8, 9]. These results suggest possible mechanisms that may be investigated using more complex models once their “blueprint” was seen in a simple conceptual model. As the study of complex systems garners increasing attention and is applied to diverse areas — from microbiology to the evolution of civilizations, passing through economics and physics — related Boolean and other discrete models are being explored more and more [10, 11, 12, 13, 14].

The purpose of this research-and-review paper is threefold: (i) to summarize and illustrate key properties and applications of BDEs; (ii) to introduce BDEs with an infinite number of variables; and (iii) to explore more fully connections between BDEs and other types of *discrete dynamical systems* (dDS). Therefore, we first describe the general form and main properties of BDEs and place them in the more general context of dDS, including cellular automata and Boolean networks (Sect. 2). Next, we summarize some applications, to climate dynamics (Sect. 3) and to earthquake physics (Sect. 4); these applications illustrate both the usefulness and beauty of BDEs. In Sect. 5 we introduce BDEs with an infinite number of variables, distributed on a spatial lattice (“partial BDEs”) and point to several ways of potentially enriching our knowledge of BDEs and extending their areas of application. Further discussion and open questions conclude the paper (Sect. 6).

2 Boolean Delay Equations (BDEs)

BDEs may be classified as *semi-discrete dynamical systems*, where the variables are discrete — typically Boolean, *i.e.* taking the values 0 (“off”) or 1 (“on”) only — while time is allowed to be continuous. As such they occupy the previously “missing corner” in the rhomboid of Fig. 1, where dynamical systems are classified according to whether their time (t) and state variables (x) are continuous or discrete.

Systems in which both variables and time are continuous are called *flows* [15, 16]

(upper corner in the rhomboid of Fig. 1). Vector fields, ordinary and partial differential equations (ODEs and PDEs), functional and delay-differential equations (FDEs and DDEs) and stochastic differential equations (SDEs) belong to this category. Systems with continuous variables and discrete time (middle left corner) are known as *maps* [17, 18] and include diffeomorphisms, as well as ordinary and partial difference equations (O Δ Es and P Δ Es).

In automata (lower corner) both the time and the variables are discrete; cellular automata (CAs) and all Turing machines (including real-world computers) are part of this group [11, 14, 19]. BDEs and their predecessors, kinetic [20] and conservative logic, complete the rhomboid in the figure and occupy the remaining middle right corner.

The connections between flows and maps are fairly well understood, as they both fall in the broader category of *differentiable dynamical systems* (DDS [15, 16, 17]). Poincaré maps (“P-maps” in Fig. 1), which are obtained from flows by intersection with a plane (or, more generally, with a codimension-1 hyperplane) are standard tools in the study of DDS, since they are simpler to investigate, analytically or numerically, than the flows from which they were obtained. Their usefulness arises, to a great extent, from the fact that — under suitable regularity assumptions — the process of suspension allows one to obtain the original flow from its P-map, which also transfers its properties to the flow.

In Fig. 1, we have outlined by labeled arrows the processes that can lead from the dynamical systems in one corner of the rhomboid to the systems in each one of the adjacent corners. Neither the processes that connect the two dDS corners, automata and BDEs, nor these that connect either type of dDS with the adjacent-corner DDS — maps and flows, respectively — are as well understood as the (P-map, suspension) pair of antiparallel arrows that connects the two DDS corners. We return to the connection between BDEs and Boolean networks in Sect. 2.6 below. The key difference between kinetic logic and BDEs is summarized in Appendix A.

2.1 General form

Given a system with n continuous real-valued state variables $\mathbf{v} = (v_1, v_2, \dots, v_n) \in \mathbb{R}^n$ for which natural thresholds $q_i \in \mathbb{R}$ exist, one can associate with each variable $v_i \in \mathbb{R}$ a Boolean-valued variable, $x_i \in \mathbb{B} = \{0, 1\}$, *i.e.*, a variable that is either “on” or “off,” by letting

$$x_i = \begin{cases} 0, & v_i \leq q_i \\ 1, & v_i > q_i \end{cases}, \quad i = 1, \dots, n. \quad (1)$$

The equations that describe the evolution of the Boolean vector $\mathbf{x} = (x_1, x_2, \dots, x_n) \in \mathbb{B}^n$ due to the time-delayed interactions between the Boolean variables $x_i \in \mathbb{B}$ are of the form:

$$\begin{cases} x_1 = f_1(x_1(t - \theta_{11}), x_2(t - \theta_{12}), \dots, x_n(t - \theta_{1n})), \\ x_2 = f_2(x_1(t - \theta_{21}), x_2(t - \theta_{22}), \dots, x_n(t - \theta_{2n})), \\ \vdots \\ x_n = f_n(x_1(t - \theta_{n1}), x_2(t - \theta_{n2}), \dots, x_n(t - \theta_{nn})). \end{cases} \quad (2)$$

Here each Boolean variable x_i is a function of time t , $x_i : \mathbb{R} \rightarrow \mathbb{B}$, and the functions $f_i : \mathbb{B}^n \rightarrow \mathbb{B}$, $1 \leq i \leq n$, are defined via Boolean equations that involve logical operators and delays. Each delay value $\theta_{ij} \in \mathbb{R}$, where $1 \leq i, j \leq n$, is the length of time it takes for a change in variable x_j to affect the variable x_i . One always can normalize delays θ_{ij} to be within the interval $(0, 1]$ so the largest one has actually the unit value; this normalization will always be assumed from now on.

Following Dee and Ghil [1], Mullhaupt [2], and Ghil and Mullhaupt [3] we consider in this section only deterministic, *autonomous* systems with no explicit time dependence. Periodic forcing is introduced in Sect. 3, and random forcing in Sect. 4. In Sects. 2–4 we consider only the case of n finite (“ordinary BDEs”), but in Sect. 5 we allow n to be infinite, with the variables distributed on a regular lattice (“partial BDEs”).

2.2 Essential theoretical results

We summarize here essential theoretical results from BDE theory; their original and complete form appears in [1, 2, 3].

We start by choosing a proper topology for the study of BDEs. Denoting by $\mathbb{B}^n[0, 1]$ the space of piecewise-constant, Boolean-valued vector functions

$$\mathbf{x}(t : 0 \leq t \leq 1) \equiv \mathbf{x} \big|_{[0,1]},$$

the system (2) can be considered as an endomorphism

$$\mathcal{F}_f : \mathbb{B}^n[0, 1] \rightarrow \mathbb{B}^n[0, 1]. \quad (3)$$

We wish to extend this endomorphism into one that acts on the solutions $\mathbf{x}(t)$ of (2):

$$\mathcal{F}_f : \mathbf{x} \big|_{[t, t+1]} \rightarrow \mathbf{x} \big|_{[t+1, t+2]}, \quad (4)$$

Changing the point of view between (2) and (4) helps us study the dynamical properties of BDEs. The space $\mathbb{B}^n[0, 1]$ equipped with the Boolean algebra and the topology induced by the L_1 metric

$$d(x, y) = \int_0^1 |x(t) - y(t)| dt, \quad (5)$$

is the *phase space* on which \mathcal{F} acts; we denote it by X . In coding theory, this metric is often called the *Hamming distance*.

In constructing solutions for a given BDE system, there is a certain similarity with the theory of real-valued delay-differential equations (DDEs) (see [21, 22, 23, 24]), as well as with that of ordinary difference equations (ODEs) ([25], [26]).

Theorem 2.1 (Existence and uniqueness) *Let $\mathbf{x}(t) \in \mathbb{B}^n[0, 1]$, be initial data with jumps at a finite number of points. Then the system (2) has a unique solution for all $t \geq 1$ and for arbitrary delays $\Theta = (\theta_{ij}) \in (0, 1]^{n^2}$.*

Sketch of Proof: The theorem can be proved by induction, constructing an algorithm that advances the solution in time and using a lemma that shows the absence of solutions with an infinite number of jumps (between 0 and 1) in any finite time interval [1]. ■

Theorem 2.2 (Continuity) *The endomorphism $\mathcal{F} : X \rightarrow X$ is continuous for given delays. Moreover, the endomorphism $\mathcal{F} : X \times [0, 1]^{n^2} \rightarrow X \times [0, 1]^{n^2}$ is continuous, where the space of delays $[0, 1]^{n^2}$ has the usual Euclidean topology.*

At this point, we need to make the critical distinction between rational and irrational delays. All BDE systems that possess only *rational* delays can be reduced in effect to finite cellular automata. Commensurability of the delays creates a partition of the time axis into segments over which state variables remain constant and whose length is an integer multiple of the delays' least common denominator (lcd). As there is only a finite number of possible assignments of two values to these segments, repetition must occur, and the only asymptotic behavior possible is eventual constancy or periodicity in time. Thus, we obtain the following

Theorem 2.3 (“Pigeon-hole” lemma) *All solutions of (2) with rational delays $\Theta \in \mathbb{Q}^{n^2}$ are eventually periodic.*

Remark. By “eventually” we mean that a finite-length transient may occur before periodicity sets in.

Dee and Ghil [1], though, found a simple system of two BDEs for which the number of jumps per unit time seemed to keep increasing with time (see Fig. 2). Complex, aperiodic behavior only arises in cellular automata for an infinite number of variables (also called sites). Thus BDEs seem to pose interesting new problems, irreducible to cellular automata. One of these, at least, is the question of which BDEs, if any, do possess solutions of increasing complexity. To answer this question, we need to classify BDEs and to study separately the effects of rational and irrational delays.

2.3 Classification

Based on the pigeon-hole lemma, Ghil and Mullhaupt [3] classified BDE systems as follows: All systems with solutions that are immediately periodic, for any set of rational delays and any initial data, are *conservative*; systems that for some initial data exhibit transient behavior before settling into eventual periodicity or quasi-periodicity are *dissipative*. The differential dynamical systems analogs are conservative (*e.g.*, Hamiltonian) dynamical systems [27, 28] versus forced-dissipative systems (*e.g.*, the well-known Lorenz [29] system). Typical examples of conservative systems occur in celestial mechanics [30], while dissipative systems are often used in modeling geophysical [31] and many other natural phenomena.

The simplest nontrivial examples of a conservative and a dissipative BDE are

$$x(t) = \bar{x}(t - 1)$$

and

$$x(t) = x(t - 1) \wedge x(t - \theta), \quad 0 < \theta < 1.$$

The Boolean operators we use are listed in Table 1. It is common to call a Boolean function $f = (f_1, \dots, f_n)$ a *connective* and its arguments x_i *channels* [32]; we shall also refer to a channel x_i simply as channel i .

Definition 2.1 *A BDE system is conservative for an open set $\Omega \subset (0, 1]^{n^2}$ of delays if for all rational delays in Ω and all initial data there are no transients. Otherwise the system is dissipative.*

Remark. We only admit initial data with a finite number of jumps.

As is usually the case in dynamical system theory, the conservative character of a BDE is tightly connected with its time *reversibility*.

Definition 2.2 *A BDE system is reversible if its time reversal also defines a system of BDEs.*

Theorem 2.4 (Conservative \Leftrightarrow Reversible) *Definitions 2.1 and 2.2 are equivalent.*

Useful algebraic criteria have been established [2, 3] for *linear* or *partially linear* systems of BDEs to be conservative. Consider the following system

$$x_i(t) = \sum_{j=1}^n c_{ij} x_j(t - \theta_{ij}) \oplus g_i(x_{j'}(t - \theta_{ij'})), \quad 1 \leq i \leq n; \quad (6)$$

here \oplus stands for addition (mod 2) in X , $c_{ij} \in \mathbb{Z}_2$, where \mathbb{Z}_2 is the *field* $\{0, 1\}$ associated with this addition, while g_i contains only such $x_{j'}$ that $c_{ij'} = 0$. The summation symbol in Eq. (6) is also understood in the sense of addition (mod 2). Note that $x \nabla y = x \oplus y$, while $x \triangle y = 1 \oplus x \oplus y$. We use the two types of symbols interchangeably, depending on the context or point of view.

Adding constants c_{i0} to the above equations corresponds to adding particular “inhomogeneous” solutions to the homogeneous linear system. All solutions of the full system can be represented as the sum of solutions to inhomogeneous and homogeneous systems. We study below only the homogeneous case.

We call a system *linear* if and only if (iff) all $g_i = 0$. Naturally, the system obtained by putting $g_i = 0$ in (6) is called the *linear part* of the BDE system. Note that this concept of linearity (mod 2) is actually very nonlinear over the field of reals \mathbb{R} , with usual addition and multiplication: it corresponds, in a sense, to the thresholding involved in Eq. (1).

First we consider the simplest case of systems with distinct rational delays in their linear part. With any such system we associate its *characteristic polynomial*

$$Q(z) = \det A(z), \quad A_{ij} = \delta_{ij} + c_{ij} z^{p_{ij}}, \quad p_{ij} = q \theta_{ij}, \quad (7)$$

where q is the lcd of all the delays θ_{ij} such that $c_{ij} \neq 0$; the degree of Q is denoted by ∂Q .

Theorem 2.5 (Conservativity for linear systems with distinct rational delays) *A linear system of BDEs is conservative for an open neighborhood Ω of a fixed n^2 -vector of distinct rational delays iff*

$$\sum_i q \sup_k \theta_{ki} = \partial Q.$$

In the case of rational delays only, we can give a first definition of *partial linearity*, namely that at least one $g_i \neq 0$ and $\partial Q \geq 2$.

Corollary 2.1 (Partially linear systems) *The same result holds for a partially linear system of BDEs with distinct rational delays.*

2.4 Solutions with increasing complexity

A natural question is whether (eventually) periodic solutions are generic in a BDE realm? Before giving a simple negative answer to this question, we need to introduce some preliminaries. To measure the complexity of a BDE solution $\mathbf{x}(t)$ that corresponds to a given set of initial data, we use the function

$$J(k) = \#\{\text{jumps of } \mathbf{x}(t) \text{ within the interval } [k, k+1)\}.$$

Lemma 2.1 (Increasingly complex solutions for linear BDEs) *All solutions (except the trivial one $x \equiv 0$) of the linear scalar BDE*

$$x(t) = x(t-1) \nabla x(t-\theta_2) \nabla \cdots \nabla x(t-\theta_\delta) \tag{8}$$

with rationally independent $0 < \theta_\delta < \cdots < \theta_2 < \theta_1 = 1$ and $\delta \geq 2$ are aperiodic and such that the lower bound for the corresponding $J(k)$ increases with time.

A simple example of this increasing complexity is given in Fig. 3, for $\delta = 2$, $\theta_2 \equiv \theta = (\sqrt{5} - 1)/2$, and a single jump in the initial data. Note that this delay is equal to the “golden ratio,” which is the most irrational number in the sense that its continued fraction expansion has the slowest possible convergence [33].

Remark. As for ODEs, a “higher-order” BDE can easily be written as a set of “first-order” BDEs (2).

A more general result holds for partially linear systems that include *irrational delays*. For such systems of the form (6), we introduce a generalized characteristic polynomial (GCP):

$$Q(\lambda) = \det A(\lambda), \quad A_{ij}(\lambda) = \delta_{ij} + c_{ij}\lambda^{t_{ij}}.$$

Clearly, this polynomial reduces to what we have in (7) if all the delays are rational and $\lambda = z^q$. The *index* ν of the GCP is defined as the number of its terms. A BDE system (6) is partially linear iff the index ν of its GCP is large enough, $\nu \geq 3$.

Theorem 2.6 (Increasingly complex solutions for partially linear BDEs) *A partially linear system of BDEs has aperiodic solutions of increasing complexity, i.e. with increasing $J(k)$, if its linear part contains $\delta \geq 2$ rationally independent delays.*

The condition in this theorem is sufficient, but not necessary. A simple counterexample is given by the third-order scalar BDE

$$x(t) = [x(t-1) \nabla x(t-\theta)] \wedge \bar{x}(t-\tau), \quad (9)$$

with θ , τ , and θ/τ irrational, and a single jump in the initial data at t_0 : $0 < 1 - \theta < 1 - \tau < t_0 < 1$. The jump function for this solution grows in time like that of Eq. (8) for $\delta = 2$, although the GCP is identically 1, so that its $\nu = 1$.

On the other hand, there exist nonlinear BDE systems with arbitrarily many incommensurable delays that have only periodic solutions. For example, all solutions of

$$\bar{x}(t) = \prod_{k=1}^n x(t - \theta_k) \quad (10)$$

are eventually periodic with period $\pi = \sum \theta_k$ for n even, and $\pi = 2 \sum \theta_k$ for n odd; the length λ of transients is bounded by $\lambda \leq \pi$. The multiplication in (10) is in the sense of the field \mathbb{Z}_2 , with $xy \equiv x \wedge y$ (see Table 1).

The increasing complexity of solutions for BDE systems that are linear (mod 2) or conservative and have irrational delays raises the question whether the jump function $J(k)$ for such solutions is bounded as time t goes to $+\infty$ or whether the jumps in Fig. 2 may accumulate. To answer this question, Dee and Ghil [1] constructed a *delay lattice* in the plane (i, j) spanned by multiples of the delay $\tau = 1$ and of the irrational delay θ , with $0 < \theta < 1$ (see their Fig. 3). By counting the number of possible jumps in a triangle lying between the τ and θ axes and the *isochron* $x + y\theta = t$ (see also Fig. 1 in [3]), these authors obtained the upper bound $J(k) \leq K t^{l-1}$, where l is, in general, the number of distinct delays and the constant K depends only on the delays Θ . This bound is the essential ingredient in proving the existence and uniqueness theorem in Sect. 2.2.

Ghil and Mullhaupt [3] obtained also a lower bound for $J(k)$, essentially showing that

$$J(k) = O(t^{\log_2(\delta+1)}) \quad (11)$$

for Eq. (8) and that $K' \log_2 \nu$ is but a lower bound for partially linear BDEs with $\delta \geq \nu - 1$. These authors, moreover, noticed the self-similarity of the pattern of jumps on the delay lattice of a linear BDE, and of a subset of the jumps, associated with the linear part, for a partially linear BDE. They also showed the log-periodic character of the jump function in Fig. 3 here (see also Fig. 7 in [3]).

Having summarized these results, we are still left with the question why Fig. 2 here, with $\theta = 0.997$ being a rational number, does exhibit increasing complexity? The question is answered by the following “main approximation theorem”.

Theorem 2.7 (Periodic approximation) *All solutions to systems of BDEs can be approximated arbitrarily well (with respect to the L_1 -norm of X) for a given finite time by the periodic solutions of a nearby system having rational delays only.*

The apparent paradox is thus solved by taking into account the length of the period obtained for a given conservative BDE and a given rational delay. As the lcd q becomes larger and larger, the solution in Fig. 3 here is well approximated for longer and longer times (see Fig. 9 of [3]); *i.e.*, the jump function can grow for a longer time, before periodicity forces it to decrease and return to a very small number of jumps per unit time.

Since the irrationals are metrically pervasive in \mathbb{R}^n , *i.e.*, they have measure one, it follows that our chances of observing solutions of conservative BDEs with infinite — or, by the approximation theorem, arbitrarily long — period are excellent. In fact, the solution shown in Fig. 2 here was discovered pretty much by chance, as soon as Dee and Ghil [1] considered a conservative system.

Ghil and Mullhaupt [3] studied, furthermore, the dependence of period length on the connective f and the delay vector Θ , as well as the degree of intermittency of self-similar solutions with growing complexity. In the latter case, we can consider each solution as a transient of infinite length. As we shall see next, such transients preclude structural stability.

2.5 Dissipative BDEs and structural stability

The concept of *structural stability* for BDEs is patterned after that for DDS. Two systems on a topological space X are said to be *topologically equivalent* if there exist a homeomorphism $h : X \rightarrow X$ that maps solution orbits from one system to those of the other. The system is *structurally stable* if it is topologically equivalent to all systems in its neighborhood [16, 34].

In discussing structural stability, we are interested in small deformations of a BDE leading to small deformations in its solution. A BDE can be changed by changing either its connective f or its delay vector Θ . Changes in f have to be measured in a discrete topology and cannot, therefore, be small. It suffices thus to consider small perturbations of the delays.

Theorem 2.8 (Structural Stability) *A BDE system is structurally stable iff all transients and all periods are bounded over some neighborhood $U \subset \mathbb{R}^{n^2}$ of its delays Θ .*

It follows that, for BDEs like for differentiable dynamical systems, conservative systems are not structurally stable in $X \times [0, 1]^{n^2}$. The conservative “vector fields,” here as there, are in some sense “rare”; for BDEs they are the three connectives \bar{x} , $x \nabla y$, and $x \Delta y$, for which the number of 0’s equals the number of 1’s in the “truth table.” Incidentally, the jump set on the delay lattice, and hence the growth of $J(k)$, is exactly the same when replacing $f(x, y) = x \nabla y$ by $f = x \Delta y$.

The structural instability and the rarity of conservative BDEs justifies studying in greater depth *dissipative* BDEs. Ghil and Mullhaupt [3] concentrated on the scalar n th-order BDE

$$x(t) = f(x(t - \theta_1), \dots, x(t - \theta_n)). \quad (12)$$

The connective f is most conveniently expressed in its *normal forms* from switching and automata theory, with $xy = x \wedge y$ and $x + y = x \vee y$. With this notation, the *disjunctive* and *conjunctive* normal forms represent f as a sum of products and a product of sums, respectively. This formalism helps prove that certain BDEs of the form (12) lead to *asymptotic simplification*, *i.e.*, after a finite transient, the solution of the full BDE satisfies a simpler BDE. An illustrative example is

$$x(t) = x(t - \theta_1) \bar{x}(t - \theta_2), \quad (13)$$

where either θ_1 or θ_2 can be the larger of the two. Asymptotically, the solutions of Eq. (13) are given by those of a simpler equation

$$x(t) = x(t - \theta_1).$$

Comparison with the asymptotic behavior of forced dissipative systems in the differentiable dynamical systems framework shows two advantages of BDEs. First, the asymptotic behavior sets in after finite (rather than infinite) time. Second, the behavior on the “inertial manifold” or “global attractor” here can be described explicitly by a simpler BDE, while this is rarely the case for a system of ODEs, FDEs, or PDEs.

Finally, one can study asymptotic stability of solutions in the L_1 -metric of X . We conclude this theoretical section by recalling that, for $0 < \theta < 1$ irrational, the solutions of

$$x(t) = x(t - \theta) x(t - 1)$$

are eventually equal to $x(t) \equiv 0$, except for $x(t) \equiv 1$, which is unstable. Likewise, for

$$x(t) = x(t - \theta) + x(t - 1),$$

$x(t) \equiv 1$ is asymptotically stable, while $x(t) \equiv 0$ is not. More generally, one has the following

Theorem 2.9 *Given rationally unrelated delays $\Theta = (\theta_k)$, the BDE*

$$x(t) = \prod_1^n x(t - \theta_k)$$

has $x(t) \equiv 0$ as an asymptotically stable solution, while for the BDE

$$x(t) = \sum_1^n x(t - \theta_k),$$

$x(t) \equiv 1$ is asymptotically stable.

To complete the taxonomy of solutions, we also note the presence of *quasi-periodic* solutions; see discussion of Eq. (6.18) in Ghil and Mullhaupt [3].

Asymptotic behavior. In summary, the following types of asymptotic behavior were observed and analyzed in BDE systems: (a) *fixed point* — the solution reaches one of a finite number of possible states and remains there; (b) *limit cycle* — the solution becomes periodic after a finite time elapses; (c) *quasi-periodicity* — the solution is a sum of several incommensurable “modes”; and (d) *growing complexity* — the solution’s number of jumps per unit time increases with time. This number grows like a positive, but fractional power of time t [1, 2], with superimposed log-periodic oscillations [3].

2.6 BDEs and Boolean networks

Given the emphasis of this special issue on complex networks, we complete here the discussion of Fig. 1 about the place of BDEs in the broader context of dynamical systems in general. Specifically, we concentrate on the relationships between BDEs and other dDS, to wit cellular automata and Boolean networks.

The formulation of BDEs was originally inspired by advances in theoretical biology, following Jacob and Monod’s discovery [35] of on-off interactions between genes, which had prompted the formulation of “kinetic logic” [20, 36, 37] and Boolean regulatory networks [38]. We briefly review the latter and discuss their relations with systems of BDEs. Kinetic logic is touched upon in Appendix A. A Boolean network is a set of Boolean variables, attached to the vertices of an oriented graph, and evolving according to Boolean rules. In particular, regular Boolean networks, in which the functions are chosen at random, but the number of inputs is the same for each node, were introduced and subsequently studied in detail by Kauffman [38, 39] for modeling interactions between genes. For recent reviews on random Boolean networks and their relations with cellular automata see [40, 41], and references therein. The most extensively studied, NK random Boolean network is a system of N variables, in which the value of each variable depends on K inputs, *i.e.* the corresponding oriented graph has connectivity $K + 1$, with K inputs and one output for each vertex, also called a node. Each node represents a given gene, which can be expressed or not, depending on the corresponding Boolean value, and each dynamical attractor corresponds to a cell type, its period being the period of its cell cycle.

The behavior is well known for the case $K = N$ and there are a number of theoretical results also for the situations $K < N$ and $K \ll N$ (in particular $K = 2$ [39, 40, 42]). Generally speaking, for small K values, there is a correspondingly small number of fixed points and limit cycles (“attractors”) in the network, whose dynamics appears “ordered,” since the attractor lengths remain finite in the limit of $N \rightarrow \infty$. For large K values, one finds instead “chaotic” behavior; in this case the difference between two almost identical initial states increases exponentially with time. The intriguing idea is that natural organisms could lie on the borderline between these two different regimes, *i.e.*

“at the edge of chaos.” Therefore, a lot of attention has been devoted to the study of such “critical” networks, in particular for $K = 2$ with a uniform distribution of the Boolean rules.

Already the problem of finding the fixed points of a generic NK random Boolean network is highly nontrivial. It has been recently addressed [43] by reformulating it in terms of the zero-energy configurations of a Hamiltonian, subject to appropriate constraints; this problem, in turn, can be handled by using statistical mechanics tools from spin glass physics [44]. The dependence of the mean number \bar{m} of attractors and of their length on the size N in critical random Boolean network is even more difficult and is still a matter of debate. The number \bar{m} seems to increase faster than any power of N in the synchronous version, in which all variables are updated at the same (discrete) time [45].

Even harder is the case of irregular random Boolean networks, in which the number of inputs K_i is also a random variable depending on the node under consideration. In this case critical, borderline behavior can also arise by choosing appropriately the weights of the Boolean functions [46]. Stability properties and their dependence on the chosen law for the K_i or on the allowed Boolean functions have been studied in [47]. *Inverse problems* for a random Boolean network try to determine which Boolean rules lead to a particular type of behavior [48].

Random Boolean networks, in which all variables are updated synchronously in discrete time, can be seen as a generalization of cellular automata [14, 40, 42], introduced by Von Neumann in the late 1940s [19]. Here the variables are distributed on a regular lattice and interact according to deterministic rule, which is usually taken to be the same for all variables. For this reason, it is well known that a finite-size random Boolean network will ultimately display either a stationary, fixed-point or a periodic behavior, exactly like a finite-size cellular automaton. Moreover, to assume that all the variables act synchronously may be too drastic a simplification for correctly modeling a number of natural systems, such as interacting genes. In order to overcome this simplification, Gershenson *et al.* [40] studied asynchronous random Boolean networks.

Klemm and Bornholdt [49] considered in detail asynchronous critical Boolean networks with $K = 2$, by introducing a weakly fluctuating delay in the response of each node. The number of synchronous attractors in the network that are stable under this perturbation increases more slowly with system size than for a fixed delay. It seems therefore that random Boolean networks in continuous time may exhibit new and possibly unexpected types of behavior. Nevertheless, in [49] variables have been prevented from switching on “too short” a time scale. The implementation of continuous time delays is thus different than in the BDE formalism and similar to the one adopted in “kinetic logic” [20, 36, 37], whose precise connections with BDEs are discussed in Appendix A. Both kinetic logic and [49] provide basically an example of an asynchronous cellular automaton.

Öktem *et al.* [50] have recently applied a BDE approach to a Boolean network of genetic interactions. In this case the time is continuous and time delays are introduced according to the BDE formalism of [1, 2, 3, 4]. Therefore, more complicated types of

behavior than in the usual Boolean network formalism can be observed, and the dynamics of the system seems to be characterized by aperiodic attractors. Still, the situation needs to be clarified further, since the authors did rule out the presence of solutions with increasing complexity by introducing, as in [49], a minimal time interval below which changes in a given variable are not permitted. For a finite number of variables, this restriction should result in an ultimately periodic behavior, though of possibly very large period, much larger than the one obtainable with usual Boolean networks, especially when considering conservative connectives and irrational delays.

In Sect. 5, we initiate the systematic study of BDE systems in the limit of an infinite number of variables, for the moment assumed to lie on a regular lattice and to interact with a given, unique, deterministic rule. This study should allow us to better understand the connections of BDEs with (infinite) cellular automata, on the one hand, and with PDEs on the other. Such a study seems also a major step in clarifying further the behavior of, possibly random, Boolean networks in continuous time.

We now turn to an illustration of BDE modeling in action, first with a climatic example and then with one from lithospheric dynamics. Both of these applications introduce new and interesting extensions to and properties of BDEs. The climatic BDE model in Sect. 3, while keeping a small number of variables, introduces variables with more than two levels, as well as periodic forcing; it shows that a simple BDE model can mimic rather well the solution set of a much more detailed model, based on nonlinear PDEs, as well as produce new and previously unsuspected results. The seismological BDE model in Sect. 4 introduces a much larger number of variables, organized in a ternary tree, as well as random forcing and state-dependent delays. This BDE model also reproduces a regime diagram of seismic sequences resembling observational data, as well as the results of much more detailed models [51, 52] based on a system of differential equations; furthermore it allows the exploration of seismic prediction methods.

3 A BDE Model for the El Niño/Southern Oscillation

The first applications of BDEs were to paleoclimatic problems. Ghil *et al.* [4] used the exploratory power of BDEs to study the coupling of radiation balance of the Earth-atmosphere system, mass balance of continental ice sheets, and overturning of the oceans' thermohaline circulation during glaciation cycles. On shorter time scales, Darby and Mysak [53] and Wohleben and Weaver [54] studied the coupling of the sea ice with the atmosphere above and the ocean below in an interdecadal Arctic and North Atlantic climate cycle, respectively. Here we describe an application to tropical climate, on even shorter, seasonal-to-interannual time scales.

The El-Niño/Southern-Oscillation (ENSO) phenomenon is the most prominent signal of seasonal-to-interannual climate variability. It was known for centuries to fishermen along the west coast of South America, who witnessed a seemingly sporadic and abrupt

warming of the cold, nutrient-rich waters that caused havoc to their fish harvests [55, 56]. Its common occurrence shortly after Christmas inspired them to name it El Niño, after the “Christ child.” Starting in the 1970s, El Niño’s climatic effects were found to be far broader than just its off-shore manifestations [55, 57]. This realization led to a global awareness of ENSO’s significance, and an impetus to attempt and improve predictions of exceptionally strong El Niño events [58].

3.1 Conceptual ingredients

The following conceptual elements are incorporated into the logical equations of our BDE model for ENSO variability.

(i) The Bjerknes hypothesis: Bjerknes [59], who laid the foundation of modern ENSO research, suggested a *positive feedback* as a mechanism for the growth of an internal instability that could produce large positive anomalies of sea surface temperatures (SSTs) in the eastern Tropical Pacific. Using observations from the International Geophysical Year (1957-58), he realized that this mechanism must involve *air-sea interaction* in the tropics. The “chain reaction” starts with an initial warming of SSTs in the “cold tongue” that occupies the eastern part of the equatorial Pacific. This warming causes a weakening of the thermally direct Walker-cell zonal circulation. As the trade winds blowing from the east subside and give way to westerly wind anomalies, the ensuing local changes in the ocean circulation encourage further SST increase. Thus the “loop” is closed and further amplification of the instability is “triggered.”

(ii) Delayed oceanic wave adjustments: Compensating for Bjerknes’s positive feedback is a *negative feedback* in the system that allows a return to colder conditions in the basin’s eastern part. During the peak of the cold-tongue warming, called the warm or El Niño phase of ENSO, westerly wind anomalies prevail in the central part of the basin. As part of the ocean’s adjustment to this atmospheric forcing, a Kelvin wave is set up in the tropical wave guide and carries a warming signal eastward; this signal deepens the eastern-basin thermocline and contributes to the positive feedback described above. Concurrently, slower Rossby waves propagate westward, and are reflected at the basin’s western “boundary,” giving rise therewith to an eastward-propagating Kelvin wave that has a cooling, thermocline-shoaling effect. Over time, the arrival of this signal erodes the warm event, ultimately causing a switch to a cold, La Niña phase.

(iii) Seasonal forcing: A growing body of work [60, 61, 62, 63, 64, 65] points to resonances between the Pacific basin’s intrinsic air-sea oscillator and the annual cycle as a possible cause for the tendency of warm events to peak in boreal winter, as well as for ENSO’s intriguing mix of temporal regularities and irregularities. The mechanisms by which this interaction takes place are numerous and intricate and their relative importance is not yet fully understood [65, 66]. We assume therefore in the present BDE model that the climatological annual cycle provides for a seasonally varying potential of event amplification.

3.2 Model variables and equations

The model [7] operates with five Boolean variables. The discretization of continuous-valued SSTs and surface winds into four discrete levels is justified by the pronounced multimodality of associated signals (see Fig. 1b of [7]).

The state of the *ocean* is depicted by SST anomalies, expressed via a combination of two Boolean variables, T_1 and T_2 . The relevant anomalous *atmospheric* conditions in the Equatorial Pacific basin are described by the variables U_1 and U_2 . The latter express the state of the trade winds. For both the atmosphere and the ocean, the first variable, T_1 or U_1 , describes the sign of the anomaly, positive or negative, while the second one, T_2 or U_2 , describes its amplitude, strong or weak. Thus, each one of the pairs (T_1, T_2) and (U_1, U_2) defines a four-level discrete variable that represents highly-positive, slightly positive, slightly negative, and highly negative deviations from the climatological mean. The *seasonal cycle's* external forcing is represented by a two-level Boolean variable S .

The atmospheric variables U_i are "slaved" to the ocean [63, 67]:

$$U_i(t) = T_i(t - \beta), \quad i = 1, 2. \quad (14)$$

The evolution of the sign T_1 of the SST anomalies is modeled according to the following two sets of delayed interactions:

(i) Extremely anomalous wind stress conditions are assumed to be necessary to generate a significant Rossby-wave signal $R(t)$, that takes on the value 1 when wind conditions are extreme at the time and 0 otherwise. By definition strong wind anomalies (either easterly or westerly) prevail when $U_1 = U_2$ and thus $R(t) = U_1(t) \Delta U_2(t)$; here Δ is the binary Boolean operator that takes on the value 1 if and only if both operands have the same value (see Sect. 2 and Table 1). A wave signal $R(t) = 1$ that is elicited at time t is assumed to re-enter the model system after a delay τ , associated with the wave's travel time across the basin. Upon arrival of the signal in the eastern equatorial Pacific at time $t + \tau$, the wave signal affects the thermocline-depth anomaly there and thus reverses the sign of SST anomalies represented by T_1 .

(ii) In the second set of circumstances, when $R(t) = 0$, and thus no significant wave signal is present, we assume that $T_1(t + \tau)$ responds directly to local atmospheric conditions, after a delay β , according to Bjerknes' hypothesis.

The two mechanisms (i) and (ii) are combined to yield:

$$T_1(t) = \{(R \wedge U_1)(t - \tau)\} \vee \{R(t - \tau) \wedge U_2(t - \beta)\}; \quad (15)$$

here the symbols \vee and \wedge represent the binary logical operators OR and AND, respectively (see Table 1).

The seasonal-cycle forcing S is given by $S(t) = S(t - 1)$; it affects the SST anomalies' amplitude T_2 through an enhancement of events when favorable seasonal conditions prevail:

$$T_2(t) = \{[S \Delta T_1](t - \beta)\} \vee \{[(S \Delta T_1) \wedge T_2](t - \beta)\}. \quad (16)$$

The time t is thus measured in units of 1 year.

The model’s principal parameters are two delays: β and τ ; they are associated with local adjustment processes and with basin-wide processes, respectively. The changes in wind conditions are assumed to lag the SST variables by a short delay β , of the order of days to weeks. For the length of the delay τ we adopt Jin’s [68] view of the delayed-oscillator mechanism and let it represent the time that elapses while combined processes of oceanic adjustment occur: it may vary from about one month in the fast-wave limit [69, 70, 71] to about two years.

3.3 Model solutions

Studying the ENSO phenomenon, we are primarily interested in the dynamics of the SST states, represented by the two-variable Boolean vector (T_1, T_2) . To be more specific, we deal with a four-level scalar variable

$$ENSO = \begin{cases} -2, & \text{extreme La Niña, } T_1 = 0, T_2 = 0, \\ -1, & \text{mild La Niña, } T_1 = 0, T_2 = 1, \\ 1, & \text{mild El Niño, } T_1 = 1, T_2 = 0, \\ 2, & \text{extreme El Niño, } T_1 = 1, T_2 = 1. \end{cases} \quad (17)$$

In all our simulations, this variable takes on the values $\{-2, -1, 1, 2\}$, precisely in this order, thus simulating the real ENSO cycles. The cycles follow the same sequence of states, although the residence time within each state changes as τ changes. The period P of a simple oscillatory solution is defined as the time between the onset of two consecutive extreme warm events, $ENSO = 2$. We use the cycle period definition to classify different model solutions (see Figs. 4–6).

(i) Periodic solutions with a single cycle (simple period). Each succession of events, or *internal cycle*, is completely phase-locked here to the seasonal cycle, *i.e.*, the warm events always peak at the same time of year. For each fixed β , as τ is increased, intervals where the solution has a simple period equal to 2, 3, 4, 5, 6, and 7 years arise consecutively.

(ii) Periodic solutions with several cycles (complex period). We describe such sequences, in which several distinct cycles make up the full period, by the parameter $\bar{P} = P/n$; here P is the length of the sequence and n is the number of cycles in the sequence. Notably, as we transition from a period of three years to a period of four years (see second inset of Fig. 4), \bar{P} becomes a nondecreasing step function of τ that takes only rational values, arranged on a Devil’s staircase.

3.4 The quasi-periodic (QP) route to chaos in the BDE model

The frequency-locking behavior observed for our BDE solutions above is a signature of the universal QP route to chaos. Its mathematical prototype is the Arnol’d circle map [15], given by the equation:

$$\theta_{n+1} = \theta_n + \Omega + 2\pi K \sin(2\pi\theta_n) \pmod{1}. \quad (18)$$

Equation (18) describes the motion of a point denoted by the angle θ of its location on a unit circle that undergoes fixed shifts by an angle Ω along the circle’s circumference. The point is also subject to nonlinear sinusoidal “corrections,” with the size of the nonlinearity controlled by a parameter K .

The solutions of (18) are characterized by their winding number

$$\omega = \omega(\Omega, K) = \lim_{n \rightarrow \infty} [(\theta_n - \theta_0)/n],$$

which can be described roughly as the average shift of the point per iteration. When the nonlinearity’s influence is small, this average shift — and hence the average period — is determined largely by Ω ; it may be rational or irrational, with the latter being more probable due to the irrationals’ pervasiveness. As the nonlinearity K is increased, “Arnol’d tongues” — where the winding number ω locks to a constant rational over whole intervals — form and widen. At a critical parameter value, only rational winding numbers are left and a complete Devil’s staircase crystallizes. Beyond this value, chaos reigns as the system jumps irregularly between resonances [72, 73].

The average cycle length \bar{P} defined for our ENSO system of BDEs is clearly analogous to the circle map’s winding number, in both its definition and behavior. Note that the QP route to chaos depends in an essential way on two parameters: Ω and K for the circle map and β and τ in our BDE model.

3.5 The “fractal sunburst”: A “bizarre” attractor

As the system undergoes the transition from an averaged period of two to three years a much more complex, and heretofore unsuspected, “fractal sunburst” structure emerges (Fig. 5, and first inset in Fig. 4). As the wave delay τ is increased, mini-ladders build up, collapse or descend only to start climbing up again. In the vicinity of a critical value ($\tau \cong 0.5$ years), the pattern’s focal point, these mini-ladders rapidly condense and the structure becomes self-similar, as each zoom reveals the pattern being repeated on a smaller scale. We call this a “bizarre attractor” because it is more than “strange”: strange attractors occur in a system’s phase space, for fixed parameter values, while this fractal sunburst appears in our model’s phase–parameter space, like the Devil’s Staircase. The structure in Fig. 4 is attracting, though, only in phase space; it is, therefore, a generalized attractor, and not just a bizarre one.

The influence of the local-process delay β , along with that of the wave-dynamics delay τ , is shown in the three-dimensional “Devil’s bleachers” (or “Devil’s terrace”, according to Jin *et al.* [63]) of Fig. 6. Note that the Jin *et al.* [62, 63] model is an intermediate model, in the terminology of modeling hierarchies [6], *i.e.* intermediate between the simplest “toy models” (BDEs or ODEs) and highly detailed models based on discretized systems of PDEs in three space dimensions, such as the general circulation models (GCMs) used in climate simulation. Specifically, the intermediate model of Jin and colleagues is based on a system of nonlinear PDEs in one space dimension (longitude along the equator). The Devil’s bleachers in our BDE model resemble fairly well those in the intermediate

ENSO model of Jin *et al.* [63]. The latter, though, did not exhibit a “fractal sunburst,” which appears, on the whole, to be an entirely new addition to the catalog of fractals [5, 74, 75].

It would be interesting to find out whether such a bizarre attractor occurs in other types of dynamical systems. Its specific significance in the ENSO problem might be associated with the fact that a broad peak with a period between two and three years appears in many spectral analyses of SSTs and surface winds from the Tropical Pacific [76, 77]. Various characteristics of the Devil’s staircase have been well documented in both observations [77, 78, 79] and GCM simulations [6, 62] of ENSO. It remains to see whether this will be the case for the fractal sunburst as well.

4 A BDE Model for Seismicity

Lattice models of systems of interacting elements are widely applied for modeling seismicity, starting from the pioneering works of Burrige and Knopoff [80], Allègre *et al.* [81], and Bak *et al.* [82]. The state of the art is summarized in [83, 84, 85, 86, 87]. Recently, colliding cascade models [8, 9, 51, 52] have been able to reproduce a wide set of observed characteristics of earthquake dynamics [88, 89, 90]: (i) the seismic cycle; (ii) intermittency in the seismic regime; (iii) the size distribution of earthquakes, known as the Gutenberg-Richter relation; (iv) clustering of earthquakes in space and time; (v) long-range correlations in earthquake occurrence; and (vi) a variety of seismicity patterns premonitory to a strong earthquake.

Introducing the BDE concept into modeling of colliding cascades, we replace the elementary interactions of elements in the system by their integral effect, represented by the delayed switching between the distinct states of each element: unloaded or loaded, and intact or failed. In this way, we bypass the necessity of reconstructing the global behavior of the system from the numerous complex and diverse interactions that researchers are only mastering by and by and never completely. Zaliapin *et al.* [8, 9] have shown that this modeling framework does simplify the detailed study of the system’s dynamics, while still capturing its essential features. Moreover, the BDE results provide additional insight into the system’s range of possible behavior, as well as into its predictability.

4.1 Conceptual ingredients

Colliding cascade models [8, 9, 51, 52] synthesize three processes that play an important role in lithosphere dynamics, as well as in many other complex systems: (i) the system has a hierarchical structure; (ii) the system is continuously loaded (or driven) by external sources; and (iii) the elements of the system fail (break down) under the load, causing redistribution of the load and strength throughout the system. Eventually the failed elements heal, thereby ensuring the continuous operation of the system.

The load is applied at the top of the hierarchy and transferred downwards, thus forming a *direct cascade of loading*. Failures are initiated at the lowest level of the hier-

archy, and gradually propagate upwards, thereby forming an *inverse cascade of failures*, which is followed by healing. The interaction of direct and inverse cascades establishes the dynamics of the system: loading triggers the failures, and failures redistribute and release the load. In its applications to seismicity, the model's hierarchical structure represents a fault network, loading imitates the effect of tectonic forces, and failures imitate earthquakes.

4.2 Model structure and parameters

(i) The model acts on a ternary tree; thus each element is a parent of three children that are siblings to each other. An element is connected to and interacts with its six nearest neighbors: the parent, two siblings, and three children.

(ii) Each element possesses a certain degree of *weakness* or *fatigue*. An element fails when its weakness exceeds a certain threshold.

(iii) The model runs in discrete time $t = 0, 1, \dots$. At each epoch a given element may be either *intact* or *failed (broken)*, and either *loaded* or *unloaded*. The state of an element e at a epoch t is defined by two Boolean functions: $s_e(t) = 0$, if an element is intact; $s_e(t) = 1$, if an element is failed; $l_e(t) = 0$, if an element is unloaded; $l_e(t) = 1$, if an element is loaded.

(iv) An element of the system may switch from one state $(s, l) \in \{0, 1\}^2$ to another under an impact from its nearest neighbors and external sources. The dynamics of the system is controlled by the time delays between the given impact and switching to another state.

(v) At the start, $t = 0$, all elements are in the state $(0, 0)$, intact and unloaded. Most of the changes in the state of an element occur in the following cycle:

$$(0, 0) \rightarrow (0, 1) \rightarrow (1, 1) \rightarrow (1, 0) \rightarrow (0, 0) \dots$$

However, other sequences are also possible, with one exception: a failed and loaded element may switch only to a failed and unloaded state, $(1, 1) \rightarrow (1, 0)$. This mimics fast stress drop after a failure.

(vi) It is supposed that all the interactions take a nonzero time. We model this by introducing four basic time delays: Δ_L , between being impacted by the load and switching to the loaded state, $(\cdot, 0) \rightarrow (\cdot, 1)$; Δ_F , between the increase in weakness and switching to the failed state, $(0, \cdot) \rightarrow (1, \cdot)$; Δ_D , between failure and switching to the unloaded state, $(\cdot, 1) \rightarrow (\cdot, 0)$; and Δ_H , between the moment when healing conditions are established and switching to the intact (healed) state, $(1, \cdot) \rightarrow (0, \cdot)$.

The duration of each particular delay, from one switch of an element's state to the next, is determined from these basic delays, depending on the state of the element as well as of its nearest neighbors during the preceding time interval (see [8] for details). This represents yet another generalization of the set of deterministic, autonomous equations (2) with fixed delays θ_{ij} : here the effective delays are variable and state-dependent.

(vii) Failures are initiated randomly within the elements at the lowest level.

The two primary delays in this system are the loading time Δ_L necessary for an unloaded element to become loaded under the impact of its parent, and the healing time Δ_H necessary for a broken element to recover.

Conservation law. The model is forced and dissipative, if we associate the loading with an energy influx. The energy dissipates only at the lowest level, where it is transferred downwards, out of the model. In any part of the model not including the lowest level energy conservation holds, but only after averaging over sufficiently large time intervals. On small intervals it may not hold, due to the discrete time delays involved in energy transfer.

Model solutions. The output of the model is a catalog of earthquakes — *i.e.*, of failures of its elements — similar to the simplest routine catalogs of observed earthquakes:

$$\mathcal{C} = (t_k, m_k, h_k), \quad k = 1, 2, \dots; \quad t_k \leq t_{k+1}. \quad (19)$$

In real-life catalogs, t_k is the starting time of the rupture; m_k is the magnitude, a logarithmic measure of energy released by the earthquake; and h_k is the vector that comprises the coordinates of the hypocenter. The latter is a point approximation of the area where the rupture started. In our BDE model, earthquakes correspond to failed elements, m_k is the level at which the failed element is situated within the model hierarchy, while the position of this element within its level is a counterpart of h_k .

4.3 Seismic regimes

A long-term pattern of seismicity within a given region is usually called a *seismic regime*. It is characterized by the frequency and irregularity of the strong earthquakes' occurrence, more specifically by (i) the Gutenberg-Richter relation, *i.e.* the time-and-space averaged magnitude–frequency distribution; (ii) the variability of this relation with time; and (iii) the maximal possible magnitude. The notion of seismic regime here is a much more complete description of seismic activity than the “level of seismicity,” often used to discriminate among regions with high, medium, low and negligible seismicity; the latter are called aseismic regions.

The seismic regime is to a large extent determined by the neotectonics of a region; this involves, roughly speaking, two factors: (i) the rate of crustal deformations; and (ii) the crustal consolidation, determining what part of deformations is realized through the earthquakes. However, as is typical for complex processes, the long-term patterns of seismicity may switch from one to another in the same region, as well as migrate from one area to another on a regional or global scale [91, 92]. Our BDE model produces synthetic sequences that can be divided into three seismic regimes, illustrated in Figs. 7–11.

Regime H: *High and nearly periodic seismicity* (top panel of Figs. 7 and 8). The fractures within each cycle reach the top level, $m = L$, where our ternary graph has height (or depth) $L = 6$. The sequence is approximately periodic, in the statistical sense of cyclo-stationarity [93].

Regime **I**: *Intermittent seismicity* (middle panel of Figs. 7 and 8). The seismicity reaches the top level for some but not all cycles, and cycle length is very irregular.

Regime **L**: *Medium or low seismicity* (lower panel of Figs. 7 and 8). No cycle reaches the top level and seismic activity is much more constant at a low or medium level, without the long quiescent intervals present in Regimes **H** and **I**.

The location of these three regimes in the plane of the two key parameters (Δ_L, Δ_H) is shown in Fig. 10.

4.4 Quantitative analysis of regimes

The quantitative analysis of model earthquake sequences and regimes is facilitated by the two measures described below.

Density of failed elements. The density $\rho(t)$ of the elements that are in a failed state at the epoch n is given by:

$$\rho(t) = [\nu_1(t) + \dots + \nu_m(t)] / m. \quad (20)$$

Here $\nu_i(t)$ is the fraction of failed elements at the i -th level of the hierarchy at the epoch t , while m is the depth of the tree. Sometimes we consider this measure averaged over a time interval, or a union of intervals, I and denote it by $\rho(I)$. The density $\rho(t)$ for the three sequences of Fig. 7 is shown in Fig. 8.

Irregularity of energy release. The second measure is the irregularity $\mathcal{G}(I)$ of energy release over the time interval I . It uses the fact that one of the major differences between regimes resides in the temporal character of seismic energy release. The measure \mathcal{G} is defined by the following sequence of steps:

(i) First, define a measure $\Sigma(I)$ of seismic activity within the time interval, or union of time ontervals, I as

$$\Sigma(I) = \frac{1}{n_I} \sum_{i=1}^{n_I} 10^{Bm_i}, \quad B = \log_{10} 3. \quad (21)$$

The summation in (21) is taken over all events within I ($t_i \in I$); n_I is the total number of such events; and m_i is the magnitude of the i -th event. The value of B equalizes, on average, the contribution of earthquakes with different magnitudes, that is from different levels of the hierarchy. In observed seismicity, $\Sigma(I)$ has a transparent physical meaning: given an appropriate choice of B , it estimates the total area of the faults unlocked by the earthquakes during the interval I [94]. This measure is successfully used in several earthquake prediction algorithms [83].

(ii) Consider a subdivision of the interval I into a set of nonoverlapping intervals of equal length $\epsilon > 0$. For simplicity we choose ϵ such that $|I| = \epsilon N_I$, where $|\cdot|$ denotes the length of an interval and N_I is an integer. Therefore, we have the following representation:

$$I = \bigcup_{j=1}^{N_I} I_j, \quad |I_k| = \epsilon, \quad k = 1, \dots, N_I; \quad I_j \cap I_k = \emptyset \text{ for } j \neq k. \quad (22)$$

(iii) For each $k = 1, \dots, N_I$ we choose such a k -subset

$$\Omega(k) = \bigcup_{i=m_1, \dots, m_k} I_i$$

that maximizes the value of the accumulated Σ :

$$\Sigma(\Omega(k)) \equiv \Sigma^*(k) = \max_{(i_1, \dots, i_k)} \{\Sigma(\cup_j I_{i_j})\}. \quad (23)$$

Here the maximum is taken over all k -subsets of the covering set (22).

(iv) Introducing the notations

$$\bar{\Sigma}(k) = \Sigma^*(k)/\Sigma(I), \quad \tau(k) = k\epsilon/|I|, \quad (24)$$

we finally define the measure of clustering within the interval I as

$$\mathcal{G}(I) = \max_{k=1, \dots, N_I} \{\bar{\Sigma}(k) - \tau(k)\}. \quad (25)$$

Figure 9 illustrates this definition by displaying the curves $\bar{\Sigma} - \tau$ vs. τ for the three synthetic sequences shown in Fig. 7; the maximum of each curve gives the corresponding value of \mathcal{G} . The more clustered the sequence, the more convex is the corresponding curve, and the larger the corresponding value of \mathcal{G} . Despite this somewhat elaborate definition, \mathcal{G} has a transparent intuitive interpretation: it equals unity for a catalog consisting of a single event (delta function, burst of energy), and it is zero for a marked Poisson process (uniform energy release). Generally, it takes values between 0 and 1 depending on the irregularity of the observed energy release.

4.5 Bifurcation diagram

Figure 11 provides a closer look at the regime diagram of Fig. 10: it illustrates the transition between regimes in the parameter plane (Δ_L, Δ_H) . To do so, Fig. 11 (a) shows a rectangular path in the parameter plane that passes through all three regimes and touches the triple point. We single out 30 points along this path; they are indicated by small circles in the figure. The three pairs of points that correspond to the transitions between regimes are distinguished by larger circles and marked in addition by letters, for example (A) and (B) mark the transition from Regime **H** to Regime **L**.

We estimate the clustering $\mathcal{G}(I)$ and average density $\rho(I)$ over the time interval I of length $2 \cdot 10^6$ time units, for representative synthetic sequences that correspond to the 30 marked points along the rectangular path in Fig. 11a. Figure 11b is a plot of $\rho(I)$ vs. $\mathcal{G}(I)$ for these 30 sequences. The values of \mathcal{G} drop dramatically, from 0.8 to 0.18, between points (A) and (B): this means that the energy release switches from highly irregular to almost uniform between Regimes **H** and **L**. This transition, however, barely changes the average density ρ of failures.

The transitions between the other pairs of regimes are much smoother. The clustering drops further, from $\mathcal{G} = 0.18$ to $\mathcal{G} \approx 0.1$, and then remains at the latter low level within Regime **L**. It increases gradually, albeit not monotonically, from 0.1 to 0.8 between points (C) and (A), on its way through regimes **I** and **H**. The increase of Δ_L along the right side of the rectangular path in Fig. 11a, between points (F) and (A), corresponds to a decrease of ρ and a slight increase of clustering \mathcal{G} , from 0.5–0.6 to ≈ 0.8 .

The transition between regimes is illustrated further in Fig. 12. Each panel shows a fragment of the six synthetic sequences that correspond to the points (A)–(F) in Fig. 11a. The sharp difference in the character of the energy release at the transition between Regimes **H** (point (A)) and **L** (point (B)) is very clear, here too. The other two transitions, from (C) to (D) and (E) to (F), are much smoother. Still, they highlight the intermittent character of Regime **I**, to which points (D) and (E) belong.

Zaliapin *et al.* [9] considered applications of these results to earthquake prediction. These authors used the simulated catalogs to study in greater detail the performance of pattern recognition methods tested already on observed catalogs and other models [83, 94, 95, 96, 97, 98, 99, 100, 101], devised new methods, and experimented with combination of different individual premonitory patterns into a collective prediction algorithm.

5 BDEs on a Lattice and Cellular Automata

While the development and applications of BDEs started about two decades ago, this is a very short time span compared to ODEs, PDEs, maps, and even cellular automata. The results obtained so far, though, are sufficiently intriguing to warrant further exploration. In this section, we provide some preliminary results on BDE systems with a large or infinite number of variables, and discuss their connections with cellular automata ([14, 19, 40, 42], see also Fig. 1 and Sect. 2.6).

Methodologically, we are led to explore “partial BDEs” in which the number n of Boolean variables is quite large or even infinite. Such systems, mentioned in passing in [2], stand in the same relation to “ordinary BDEs,” explored so far, as PDEs do to ODEs. The classification of what we could call now *ordinary* BDEs into conservative and dissipative (Sect. 2) suggests that *partial* BDEs of different types can exist as well.

In the following we sum up a few results that we obtained along these lines. We consider Boolean functions $u(x, t) = 0, 1$ of $x \in \mathbb{R}$ and $t \in \mathbb{R}^+$, *i.e.* we are studying the spatially one-dimensional (1-D) case. The first step is to clarify what is the correct “BDE equivalent” of partial derivatives, and we started by studying possible candidates for *hyperbolic* and *parabolic* partial BDEs. Intuitively, these should correspond to infinite-dimensional (in phase space) generalizations of conservative and dissipative BDEs, respectively (see Sects. 2.3 and 2.5). As a first attempt, one can replace partial derivatives by the “exclusive or” operator ∇ (see Table 1).

5.1 Hyperbolic BDEs

With this interpretation of ∂_t and ∂_x , one gets a partial BDE of *hyperbolic* type, analogous to the simplest wave equation

$$u(x, t + k) \nabla u(x, t) = u(x \pm h, t) \nabla u(x, t) \quad h, k \in (0, 1], \quad (26)$$

defined on the lattice (ih, jk) for $(i, j) \in \mathbb{N}^2$. The general solution of the pure Cauchy problem for Eq. (26) is

$$u(x, t + k) = u(x \pm h, t) \quad \forall h, k \in (0, 1]; \quad (27)$$

it displays the expected behavior of a “wave” propagating in the (x, t) plane (not shown). This propagation is, respectively, from right to left for increasing times when the “plus” sign is chosen or in the opposite direction for the “minus” sign in Eqs. (26),(27).

Interestingly, we find that the apparently very similar equation, which could also be considered a reasonable candidate for hyperbolic BDEs,

$$u(x, t + k) \nabla u(x, t) = u(x - h, t) \nabla u(x + h, t), \quad h, k \in (0, 1], \quad (28)$$

has a very different behavior. Note that Eq. (26) corresponds to well-balanced first-order approximations of both ∂_t and ∂_x , while the ∂_x in Eq. (28) is a second-order accurate approximation of ∂_x [102]. By “multiplying” both sides of (28) by $\nabla u(x, t)$, one finds

$$u(x, t + k) = u(x - h, t) \nabla u(x, t) \nabla u(x + h, t). \quad (29)$$

We recall that the Boolean binary operator ∇ is associative, since it corresponds to addition (mod 2), and hence no parentheses are needed on the right-hand side of Eq. (29).

At this point, we recall the definition of the *elementary* 1-D cellular automaton studied in detail by Wolfram [103]. Such an automaton, which we shall call ECA for simplicity, is a set of Boolean variables u_i distributed on a regular 1-D lattice $\{x_i = ih, -N \leq i \leq N\}$, that evolve in synchronous steps, according to a set of Boolean rules; these rules involve only the variable u_i at the site x_i and several immediate neighbors, typically $u_{i\pm 1}$. Note that the exact number n of BDEs that we can associate with such an ECA depends on the boundary conditions: $n = 2N + 1$ if these are periodic, but it can be lower or higher if one uses Dirichlet or Neumann boundary conditions.

In an ECA that involves only the nearest right and left neighbors $u_{i\pm 1}$, the single rule valid at all sites can be described by a binary string that summarizes the truth table of the rule: ordering the values of the inputs (u_{i-1}, u_i, u_{i+1}) in decreasing order, from 111 to 000, one gets $2^3 = 8$ binary digits, 1 or 0, for each possible output. Thus, if we consider Eq. (29) for $h = k = 1$ as the representation of an ECA, the 8-digit string that characterizes the 3-site rule on its right-hand side is 10010110; for brevity one can replace each such 8-digit binary number by its decimal representation, which yields, in this case, rule 150 [103]. We also recall that, for N finite, the ECA version of our pigeon-hole lemma (Theorem 2.3 in Sect. 2.2) states that all solutions of such an automaton have to

become stationary or purely periodic after a finite number of time steps. For N infinite, however, rule 150 yields interesting behavior, with self-similar, fractal patterns embedded in its spatio-temporal structure.

We studied therefore in detail the simple case $h = k = 1$ of Eq. (29), where in the initial state the Boolean variables u_i are assumed constant for $0 \leq \tau < 1$ and $x_i - h < x \leq x_i$. We thus verify merely that our partial BDEs do generate all known classes of ECA behavior, while less trivial BDEs do yield very distinct behavior.

For any partial BDE, one can formulate both a pure Cauchy problem, for u given on $-\infty < x_i < \infty, i \in \mathbb{N}$, and a space-periodic initial boundary value problem (IBVP), *i.e.* $i = 0, \dots, N$ with $u(x_{i+N}, 0) = u(x_i, 0)$. The behavior of Eq. (29) in both cases can be obtained from the evolution of the corresponding ECA, which we show in Fig. 13a. This rule exhibits the important simplifying feature of “additive superposition” [103], as evident from Fig. 13b, where the collision of two “waves” is plotted. Correspondingly, we find that, in the IBVP case, the solutions can behave very differently, depending on the value of N and on the initial state $u(x_i, 0), i = 0, \dots, N$.

We limited the preliminary study here to the case of N being an integer multiple of the spatial period T_x of the initial state $u(x_i, 0)$. In this case — apart from the presence of possible fixed points, in particular for $T_x \leq 3$ — the solutions of Eq. (29) display the longest periods when $x_0 = x_{T_x} = 1$ and $x_i = 0$ for i not a multiple of T_x . In agreement with the ECA results for rule 150 [103], we find that our solutions are immediately periodic for T_x not a multiple of three, whereas there is a transient when $T_x = 3p, p \in \mathbb{N}$; this transient is of length 1 for T_x odd and of length 2^{j-1} , where 2^j is the largest power of two which divides T_x , otherwise. The presence of transients corresponds to “dissipative” behavior (see Sects. 2.3 and 2.5), which can be associated with the second-order approximation of ∂_x made in Eqs. (28,29) [102]. The ECA with rule 150 belongs to the third class in Wolfram’s [103, 104] classification, in which evolution for $N \rightarrow \infty$ can lead to chaotic patterns; therefore, even if its behavior is predictable from the knowledge of the initial state, the length of the period can increase rapidly with N . In particular, one finds a time period already as long as $T_t = 511$ for $T_x = 19$ (see Fig. 14).

The behavior would clearly not be periodic in time in the limit of $N \rightarrow \infty$ when choosing an initial state that is not periodic in space. In order to illustrate this point, we present in Fig. 15 the results for Eq. (29) with a random initial state of length $N = 100$; these results do not show any “recurrent pattern,” apart from the expected [14, 42] appearance of the characteristic “triangles.”

5.2 Parabolic BDEs

The *parabolic* BDE case, which is the analogous of the heat equation $\partial_t u = \partial_{xx} u$, looks still more intriguing. One can consider on the right-hand side either a spatial connective that is dissipative without being of second order,

$$u(x, t + k) \nabla u(x, t) = u(x + h, t) \wedge u(x - h, t), \quad (30)$$

or apply two times the ∇ operator, yielding

$$u(x, t+k)\nabla u(x, t) = [u(x-h, t)\nabla u(x, t)]\nabla [u(x, t)\nabla u(x+h, t)] = u(x-h, t)\nabla u(x+h, t). \quad (31)$$

For $h = k = 1$, our parabolic BDE (31) corresponds to the ECA with rule 90 [103]. This ECA has a similar behavior to the previously considered rule 150; in particular, it displays the same property of “additive superposition” and lies in the same universality class. It seems, therefore, that to use a second-order approximation for ∂_x or to approximate ∂_{xx} to first order gives partial BDEs with the same kind of behavior. Hence, both Eqs. (29) and (31) appear to fall into the dissipative, parabolic class of partial BDEs.

On the other hand, Eq. (30) can be shown to be equivalent, for $h = k = 1$, to the ECA with rule 108, which is in the second class of Wolfram’s classification [103]; here the evolution leads to a set of spatially separated, stable or periodic structures and it does not display chaotic behavior. Nevertheless, different starting configurations will generally give different long-time patterns (not shown). Interestingly, replacing the AND operator in Eq. (30) with the OR operator, one gets, for k/h rational, the ECA with rule 54, which belongs to the first class [103, 104] and whole evolution leads to a “homogeneous” state, independent of the starting one (not shown).

5.3 Future work

Our results on classifying finite BDE systems, on the one hand, and our point of view of replacing partial derivatives in PDEs by Boolean operators, on the other, seem to provide interesting insights into the correspondence between partial BDEs and PDEs. In Sects. 5.1 and 5.2 we have only considered the trivial case of $h = k = 1$, in which close correspondence exists between our partial BDEs and ECAs. This correspondence simply sheds new light on the known results of certain cellular automata.

The case of nonconstant starting data in the initial interval, and the more general one of irrational h, k values are left for future studies. To give an idea of the possible outcomes, consider, for simplicity the solution of Eq. (26) with initial data of the Riemann type, having a single jump in u at $x = 0$ and $t = 1/2 < k$, say, *i.e.*, $u = 1$ for $-\infty < x \leq 0$ and $0 \leq t \leq 1/2$, and $u = 0$ in the rest of the initial strip, $\{(x, t) : -\infty < x < \infty, t < k\}$. The obvious conjecture is that, for k/h rational, the solution will still be a right- or left-traveling wave, depending on the sign taken in the right-hand side of the partial BDE. Hence, certain x -periodic IBVPs will also be well posed and additive superposition will provide insight into solution behavior, which might include certain solutions that exhibit both t - and x -periodicity.

For k/h irrational, however, we strongly suspect that solutions of the hyperbolic BDE (26) will increase in complexity with respect to both $|x|$ and t , as well as along most rays $x/t = \text{const}$. If so, this would provide us with an even richer metaphor for evolution than either ordinary BDEs or cellular automata. The role of *characteristics* will be played here by the resonant lines $(x/mh) + (t/nk) = \text{const.}$, with m and n integer.

In the parabolic case (30) we conjecture instead that the solution $u \equiv 0$ will be asymptotically stable, when k/h is irrational, at least for large $|x|$. Conversely, $u \equiv 1$ should be asymptotically stable when replacing the AND operator by OR in Eq. (30); see Theorem 2.9 in Sect. 2.5. However, nontrivial solutions of parabolic problems could be obtained in the presence of forcing, like for PDEs.

6 What Next?

The most promising development in the theory and applications of BDEs seems to be the extension to an infinite, or very large, number of variables as discussed in Sect. 4 ($n = 2 \times (3^8 - 1)/2 \cong 6 \times 10^3$) and Sect. 5 ($n \rightarrow \infty$). Inhomogeneous partial BDEs can be easily handled by introducing “variable coefficients,” *i.e.* multiplication of the right-hand side by site-dependent Boolean variables or functions.

Another important possibility is the randomization of various aspects of the BDE formulation. Wright *et al.* [105] have already considered ensemble averaging over BDE solutions with randomized initial data, while Zaliapin *et al.* [8, 9] have considered random forcing. It would be even more interesting to consider the random perturbation of delays, first in the ordinary and then in partial BDEs; see also work along these lines in Boolean networks [49].

Next, an important but harder goal of the theory will be to develop *inverse methods*. In other words, given the behavior of a complicated natural system, which can be described in a first approximation by a finite number of discrete variables, one would like to discover a good connective linking these variables and yielding the observed behavior for plausible values of the delays. In this generality, the inverse problem for ODEs, say, is clearly intractable. But some of the direct results obtained so far — see, for instance, the asymptotic-simplification results in Sect. 2.5 — hold promise for BDEs, at least within certain classes and with certain additional conditions. Intuitively, the behavior of BDEs, although surprisingly rich, is more rigidly constrained than that of flows. Certain inverse-modeling successes have also been reported for cellular automata; see [14] and references there.

From the point of view of applications, BDEs have been applied fairly extensively by now to climate dynamics [4, 53, 54, 105, 106, 107, 108] and are making significant inroads into solid-earth geophysics [8, 9]. Most interesting are recent applications to the life sciences (Neumann and Weisbuch [109, 110], Gagneur and Casari [13], Öktem *et al.* [50]), which represent in a sense a return to the motivation of the geneticist René Thomas, originator of kinetic logic [20, 36, 37]; see also Sect. 2.6 and Appendix A for details.

BDEs may be suited for the exploration of poorly understood phenomena in the socio-economic realm as well. Moreover, the robustness of fairly regular solutions in a wide class of BDEs, for many sets of delays and a variety of initial states, suggests interesting applications to certain issues in massively parallel computations.

Acknowledgements. It is a pleasure to thank the organizers of the International Workshop and Seminar “Dynamics on Complex Networks and Applications” (DYONET 2006), especially Juergen Kurths and Manuel Matias, for the opportunity to interact with the participants, as well as with the members of the Max-Planck-Institut für Physik Komplexer Systeme in Dresden, Germany, and prepare this research-and-review paper. We are indebted to all the collaborators who helped us formulate, analyze, and apply BDEs: D. P. Dee (European Centre for Medium-Range Weather Forecast, Reading, U.K.), V. I. Keilis-Borok (IGPP, UCLA; and MITPAN, Moscow), A. P. Mullhaupt (Wall Street), P. Pestiaux (Total, France), and A. Saunders (Magnet High School, Van Nuys, CA). Comments and suggestions by E. Simonnet and G. Weisbuch and two anonymous reviewers have helped improve the original manuscript. This work was supported by NSF Grants ATM-0082131 and ATM-0327558, and by the European Commission’s Project no. 12975 (NEST) ”Extreme Events: Causes and Consequences (E2-C2).”

A BDEs and Kinetic Logic

A mathematical model closely related to BDEs was formulated by R. Thomas [37] in a slightly different form. The difference can best be explained in terms of “memorization variables” $x_{ij}(t) = x_j(t - \theta_{ij})$. In our formulation $x_{ij}(t)$ is a purely delayed state variable; that is, $x_{ij}(t)$ is determined only by the state of the system at time $t - \theta_{ij}$. Thomas allows the memorization variable $x_{ij}(t)$ to depend on the state of the system up to time t : when a change takes place in any variable x_k in the time interval $(t - \theta_{ij}, t)$, then the memorization variable x_{ij} may change also.

Specifically, if for some $t' \in (t - \theta_{ij}, t)$ the state of the system is such that

$$x_j(t') = f_j(x_1(t'), \dots, x_n(t')) \neq x_j(t - \theta_{ij}), \quad (32)$$

then the memorization variable $x_{ij}(t)$, previously equal to $x_j(t - \theta_{ij})$, is changed to

$$x_{ij}(t) = x_j(t'). \quad (33)$$

The adjustment of the variables x_{ij} is in effect selectively erases some of the memory of the system. The resulting solutions are usually simpler and hence easier to study than the typical solution of our BDEs. Referring to the examples shown in Figs. 2 and 3 here, the increasing complexity of the solution reflects the fact that the memory of the system contains more and more information as time goes on.

In Thomas’s kinetic logic formulation, such solutions of increasing complexity cannot arise. They are due precisely to the “conflicts” between variable values that were avoided on purpose in kinetic logic [13]. A similar policy of eliminating behavior that is too complicated and thus too hard to capture numerically appears in [49, 50].

References

- [1] Dee D., and M. Ghil, 1984. Boolean difference equations, I: Formulation and dynamic behavior. *SIAM J. Appl. Math.*, 44, 111–126.
- [2] Mullhaupt, A. P., 1984. Boolean Delay Equations: A Class of Semi-Discrete Dynamical Systems. Ph. D. thesis, New York University [published also as Courant Institute of Mathematical Sciences Report CI-7-84, 193 pp.]
- [3] Ghil, M., and A. P. Mullhaupt, 1985. Boolean delay equations. II: Periodic and aperiodic solutions. *J. Stat. Phys.*, 41, 125–173.
- [4] Ghil, M., A. P. Mullhaupt, and P. Pestiaux, 1987. Deep water formation and Quaternary glaciations. *Clim. Dyn.*, 2, 1–10.
- [5] Mandelbrot, B. 1982. *The Fractal Geometry of Nature*. W. H. Freeman, 480 pp.
- [6] Ghil, M., and A. W. Robertson, 2000. Solving problems with GCMs: General circulation models and their role in the climate modeling hierarchy. In D. Randall (Ed.) *General Circulation Model Development: Past, Present and Future*, Academic Press, San Diego, pp. 285–325.
- [7] Saunders, A., and M. Ghil, 2001. A Boolean delay equation model of ENSO variability. *Physica D*, 160, 54–78.
- [8] Zaliapin, I., V. Keilis-Borok, and M. Ghil, 2003a. A Boolean delay equation model of colliding cascades. Part I: Multiple seismic regimes. *J. Stat. Phys.*, 111, 815–837.
- [9] Zaliapin, I., V. Keilis-Borok, and M. Ghil, 2003b. A Boolean delay equation model of colliding cascades. Part II: Prediction of critical transitions. *J. Stat. Phys.*, 111, 839–861.
- [10] Cowan, G. A., D. Pines and D. Melzer, Eds., 1994. *Complexity: Metaphors, Models and Reality*. Addison-Wesley, Reading, Mass.
- [11] Gutowitz, H., 1991. *Cellular Automata: Theory and Experiment*. MIT Press, Cambridge, MA.
- [12] Kauffman, S. A., 1995. *At Home in the Universe: The Search for Laws of Self-Organization and Complexity*. Oxford University Press, New York.
- [13] Gagneur, J., and G. Casari, 2005. From molecular networks to qualitative cell behavior. *FEBS Letters*, 579 (8), Special Issue, 1867–1871.
- [14] Wolfram, S., 1994. *Cellular Automata and Complexity: Collected Papers*. Addison-Wesley, Reading, Mass.

- [15] Arnol'd, V. I., 1983. *Geometrical Methods in the Theory of Ordinary Differential Equations*. Springer-Verlag, New York.
- [16] Smale, S., 1967. Differentiable dynamical systems. *Bull. Amer. Math. Soc.*, 73, 747–817.
- [17] Collet, P., and J.-P. Eckmann, 1980. *Iterated Maps on the Interval as Dynamical Systems*. Birkhäuser Verlag, Basel/Boston/Birkhäuser.
- [18] Hénon, M., 1966. La topologie des lignes de courant dans un cas particulier. *C. R. Acad. Sci. Paris.*, 262, 312–414.
- [19] Von Neumann, J., 1966. *Theory of Self-Reproducing Automata*, University of Illinois Press, Urbana, Illinois.
- [20] Thomas, R., Ed., 1979. *Kinetic Logic: A Boolean Approach to the Analysis of Complex Regulatory Systems*, Springer-Verlag, Berlin/Heidelberg/New York, 507 pp.
- [21] Bhattacharyya, K. and M. Ghil, 1982. Internal variability of an energy-balance model with delayed albedo effects. *J. Atmos. Sci.*, 39, 1747–1773.
- [22] Driver, R.D., 1977. *Ordinary and Delay Differential Equations*, Applied Mathematical Sciences Series, 20, Springer-Verlag, New York.
- [23] Hale, J., 1971. *Functional Differential Equations*. Springer-Verlag, New York.
- [24] McDonald, N., 1978. *Time Lags in Biological Models*. Springer-Verlag, New York.
- [25] Bellman, R. and Cooke, K. L., 1963. *Differential-Difference Equations*. Academic Press, New York.
- [26] Isaacson, E. and Keller, H. B., 1966. *Analysis of Numerical Methods*. John Wiley, New York.
- [27] Guckenheimer, J., and P. Holmes, 1997. *Nonlinear Oscillations, Dynamical Systems and Bifurcations of Vector Fields*. 3rd ed, Springer-Verlag, New York.
- [28] Lichtenberg, A. J., and M. A. Liebermann, 1983. *Regular and Stochastic Motion*, Springer-Verlag, New York/Heidelberg/Berlin, 499 pp.
- [29] Lorenz, E. N., 1963. Deterministic nonperiodic flow. *J. Atmos. Sci.*, 20, 130–141.
- [30] Arnol'd, V. I., 1978. *Mathematical Methods of Classical Mechanics*, Springer-Verlag, New York, 462 pp.
- [31] Ghil, M., and S. Childress, 1987. *Topics in Geophysical Fluid Dynamics: Atmospheric Dynamics, Dynamo Theory and Climate Dynamics*, Springer-Verlag, New York/Berlin/London/Paris/ Tokyo, 485 pp.

- [32] Arnold B. H., 1962. *Logic and Boolean Algebra*. Prentice-Hall, Englewood Cliffs, New Jersey.
- [33] Khinchin, A. Ya., 1964. *Continued Fractions*, Univ. of Chicago Press, Chicago, IL.
- [34] Andronov, A. and L. Pontryagin, 1937. Systèmes grossiers. *Dokl. Akad. Nauk. USSR*, 14, 247–251.
- [35] Jacob, F. and Monod, J., 1961. Genetic regulatory mechanisms in the synthesis of proteins. *J. Mol. Biol.*, 3, 318–356.
- [36] Thomas, R., 1973. Boolean formalization of genetic control circuits. *J. Theoret. Biol.*, 42, 563–585.
- [37] Thomas, R., 1978. Logical analysis of systems comprising feedback loops. *J. Theoret. Biol.*, 73, 631–656.
- [38] Kauffman, S. A., 1969. Metabolic stability and epigenesis in randomly constructed genetic nets. *J. Theor. Biol.* 22, 437–467.
- [39] Kauffman, S.A., 1993. *The origin of order*, Oxford University Press.
- [40] Gershenson, C., 2004. Introduction to random Boolean networks, *nlin.AO/0408006*, in M. Bedau, P. Husbands, T. Hutton, S. Kumar and H. Suzuchi (eds.) *Workshop and Tutorial Proceeding, Ninth International Conference on the Simulation and Synthesis of Living Systems (ALife IX)*, 160–173.
- [41] Aldana Gonzalez, M., Coopersmith, S. and Kadanoff, L.P., 2003. In *Perspectives and Problems in Nonlinear Science, A Celebratory Volume in Honor of Lawrence Sirovich*, Applied Mathematical Science, Springer Verlag, New York, pp 23–89.
- [42] Weisbuch, G., 1991. *Complex Systems Dynamics: An Introduction to Automata Networks* Lecture Notes Volume II, Santa Fe Institute, Studies in the Sciences of Complexity. Addison Wesley, Redwood City, CA.
- [43] Correale, L., Leone, M., Pagnani, A., Weigt, M., and Zecchina, R., 2006. Core percolation and onset of complexity in Boolean networks *Phys. Rev. Lett.* **96**, 018101.
- [44] Mézard, M., Parisi, G., and Zecchina, R., 2002. Analytic and algorithmic solution of satisfiability problems, *Science* **297**, 812–815.
- [45] Mihaljev, T., and Drossel, B., Scaling in a general class of critical random Boolean networks, *cond-mat/0606612*.
- [46] Albert, R., and Barabási, A.-L., 2002. Statistical mechanics of complex networks, *Rev. Mod. Phys.* **74**, 47–97.

- [47] Kauffman, S., Peterson, C., Samuelsson, B., and Troein, C., 2004. Genetic networks with canalizing Boolean rules are always stable. *Proc. Natl. Ac. Sci. USA* **101**, 17102–17107.
- [48] Mesot, B., and Teuscher, C. 2005. Deducing local rules for solving global tasks with random Boolean networks. *Physica D*, 211 (1-2), 88–106.
- [49] Klemm, K., and Bornholdt, S., 2005. Stable and unstable attractors in Boolean networks. *Phys. Rev. E* **72**, 055101.
- [50] Öktem, H., R. Pearson, and K. Egiazarian, 2003. An adjustable aperiodic model class of genomic interactions using continuous time Boolean networks (Boolean delay equations) *Chaos*, 13, 1167–1174.
- [51] Gabrielov, A., V. Keilis-Borok, I. Zaliapin, and W. I. Newman, 2000. Critical transitions in colliding cascades, *Phys. Rev. E*, 62, 237–249.
- [52] Gabrielov, A.M., I. V. Zaliapin, V. I. Keilis-Borok, and W. I. Newman, 2000. Colliding cascades model for earthquake prediction. *J. Geophys. Intl.*, 143, 427–437.
- [53] Darby, M. S., and L. A. Mysak, 1993. A Boolean delay equation model of an interdecadal Arctic climate cycle. *Climate Dyn.*, 8, 241–246.
- [54] Wohleben, T.M.H. and A.J. Weaver, 1995. Interdecadal climate variability in the subpolar North Atlantic. *Clim. Dynam.*, 11(8), 459–467.
- [55] Diaz, H. F., and V. Markgraf, Eds., 1992. *El Niño: Historical and Paleoclimatic Aspects of the Southern Oscillation*. Cambridge Univ Press, New York.
- [56] Philander, S. G. H., 1990. *El Niño, La Niña, and the Southern Oscillation*, Academic Press, San Diego.
- [57] Glantz, M. H., R. W. Katz, and N. Nicholls, Eds. 1991. *Teleconnections Linking Worldwide Climate Anomalies*. New York: Cambridge Univ. Press.
- [58] Latif, M., T. P. Barnett, M. Flügel, N. E. Graham, J. -S. Xu, and S. E. Zebiak, 1994. A review of ENSO prediction studies. *Clim. Dyn.*, 9, 167–179.
- [59] Bjerknes, J., 1969, Atmospheric teleconnections from the equatorial Pacific. *Mon. Wea. Rev.*, 97, 163–172.
- [60] Chang, P., B. Wang, T. Li and L. Ji, 1994. Interactions between the seasonal cycle and the Southern Oscillation: Frequency entrainment and chaos in intermediate coupled ocean-atmosphere model. *Geophys. Res. Lett.* 21, 2817–2820.

- [61] Chang, P., L. Ji, B. Wang and T. Li, 1995. Interactions between the seasonal cycle and El Niño - Southern Oscillation in an intermediate coupled ocean-atmosphere model. *J. Atmos. Sci.* 52, 2353–2372.
- [62] Jin, F.-f., J. D. Neelin, and M. Ghil, 1994. El Niño on the Devil’s Staircase: Annual subharmonic steps to chaos, *Science*, 264, 70–72.
- [63] Jin, F.-f., J. D. Neelin, and M. Ghil, 1996. El Niño/Southern Oscillation and the annual cycle: Subharmonic frequency locking and aperiodicity, *Physica D*, 98, 442–465.
- [64] Tziperman, E., L. Stone, M. Cane, and H. Jarosh, 1994. El Niño chaos: Overlapping of resonances between the seasonal cycle and the Pacific ocean-atmosphere oscillator. *Science*, 264, 72–74.
- [65] Tziperman, E., M. A. Cane and S. E. Zebiak, 1995. Irregularity and locking to the seasonal cycle in an ENSO prediction model as explained by the quasi-periodicity route to chaos. *J. Atmos. Sci.*, 50, 293–306.
- [66] Battisti, D. S., 1988. The dynamics and thermodynamics of a warming event in a coupled tropical atmosphere/ocean model. *J. Atmos. Sci.* 45, 2889–2919.
- [67] Neelin, J. D., M. Latif, and F.-f. Jin, 1994. Dynamics of coupled ocean-atmosphere models: the tropical problem. *Annu. Rev. Fluid Mech.*, 26, 617–659.
- [68] Jin, F.-f., 1996. Tropical ocean-atmosphere interaction, the Pacific cold tongue, and the El-Niño-Southern Oscillation. *Science*, 274, 76–78.
- [69] Jin F.-f., and J. D. Neelin, 1993. Modes of interannual tropical ocean-atmosphere interaction-A unified view. I. Numerical results. *J. Atmos. Sci.*, 50, 3477–3503.
- [70] Jin, F.-f., and J. D. Neelin, 1993. Modes of interannual tropical ocean-atmosphere interaction-A unified view. II. Analytical results in fully coupled cases. *J. Atmos. Sci.*, 50, 3504–3522.
- [71] Jin, F.-f., and J. D. Neelin, 1993. Modes of interannual tropical ocean-atmosphere interaction - A unified view. III. Analytical results in fully coupled cases. *J. Atmos. Sci.*, 50, 3523–3540.
- [72] Jensen, M. H., P. Bak, and T. Bohr, 1984. Transition to chaos by interaction of resonances in dissipative systems. Part I. Circle maps. *Phys. Rev. A*, 30, 1960–1969.
- [73] Schuster, H. G., 1988. *Deterministic Chaos: An Introduction*. Physik-Verlag, Weinheim.
- [74] Peitgen, H.-O., and P. Richter, 1986. *The Beauty of Fractals*, Springer-Verlag, Heidelberg.

- [75] Peitgen, H., H. Juergens and D. Saupe, 1992. *Chaos and Fractals: New Frontiers of Science*, Springer-Verlag, New York.
- [76] Rasmusson, E. M., X. Wang, and C. F. Ropelewski, 1990. The biennial component of ENSO variability. *J. Marine Syst.*, 1, 71–96.
- [77] Jiang, N., J. D. Neelin and M. Ghil, 1995. Quasi-quadrennial and quasi-biennial variability in the equatorial Pacific. *Clim. Dyn.*, 12, 101–112.
- [78] Moron, V., R. Vautard, and M. Ghil, 1998. Trends, interdecadal and interannual oscillations in global sea-surface temperatures, *Clim. Dyn.*, 14, 545–569.
- [79] Yiou, P., D. Sornette, and M. Ghil, 2000. Data-adaptive wavelets and multi-scale SSA, *Physica D*, 142, 254–290.
- [80] Burridge, R., and L. Knopoff, 1967. Model and theoretical seismicity, *Bull. Seism. Soc. Am.*, 57, 341–371.
- [81] Allègre, C. J., J. L. Le Mouel, and A. Provost, 1982. Scaling rules in rock fracture and possible implications for earthquake prediction. *Nature*, 297, 47–49.
- [82] Bak, P., C. Tang, and K. Wiesenfeld, 1988. Self-organized criticality. *Phys. Rev. A*, 38, 364–374.
- [83] Keilis-Borok, V. I., 2002. Earthquake prediction: State-of-the-art and emerging possibilities. *Annu. Rev. Earth Planet. Sci.*, 30, 1–33.
- [84] Keilis-Borok, V. I. and Shebalin, P. N., Eds., 1999. Dynamics of lithosphere and earthquake prediction. *Phys. Earth Planet. Int.*, 111, 179–330.
- [85] Newman, W. I., A. M. Gabrielov, and D. L. Turcotte, Eds., 1994. *Nonlinear Dynamics and Predictability of Geophysical Phenomena*, Geophys. Monographs Ser. 83, American Geophysical Union, Washington, DC.
- [86] Rundle, J. B., D. L. Turcotte, and W. Klein, Eds., 2000. *Geocomplexity and the Physics of Earthquakes*. American Geophysical Union, Washington, DC.
- [87] Turcotte, D. L., W. I. Newman, and A. M. Gabrielov, 2000. A statistical physics approach to earthquakes. In: J. B. Rundle, D. L. Turcotte, and W. Klein, Eds., *Geocomplexity and the Physics of Earthquakes*. American Geophysical Union, Washington, DC, pp. 83–96.
- [88] Keilis-Borok, V. I., 1996. Intermediate-term earthquake prediction. *Proc. Natl. Acad. Sci. USA*, 93, 3748–3755.
- [89] Scholz, C. H., 1990. *The Mechanics of Earthquakes and Faulting*. Cambridge University Press, Cambridge.

- [90] Turcotte, D. L., 1997. *Fractals and Chaos in Geology and Geophysics*, 2nd ed., Cambridge University Press, Cambridge.
- [91] Press, A. and Allen, C., 1995. Pattern of seismic release in the southern California region. *J. Geophys. Res.*, 100, 6421–6430.
- [92] Romanowicz, B., 1993. Spatiotemporal patterns in the energy-release of great earthquakes, *Science*, 260, 1923–1926.
- [93] Mertins, A., 1999. *Signal Analysis: Wavelets, Filter Banks, Time-Frequency Transforms and Applications*. John Wiley and Sons, Chichester.
- [94] Keilis-Borok, V. I. and Malinovskaya, L. N., 1964. One regularity in the occurrence of strong earthquakes. *J. Geophys. Res.*, 69, 3019–3024.
- [95] Jaume S. C., Sykes, L. R. 1999. Evolving towards a critical point: A review of accelerating seismic moment/energy release prior to large and great earthquakes, *Pure Appl. Geophys.*, 155, 279–306.
- [96] Keilis-Borok, V. I., 1994. Symptoms of instability in a system of earthquake-prone faults, *Physica D*, 77, 193–199.
- [97] Pepke, G. F., Carlson, J. R., and Shaw, B. E., 1994. Prediction of large events on a dynamical model of fault. *J. Geophys. Res.*, 99, 6769–6788.
- [98] Molchan, G. M., Dmitrieva, O. E., Rotwain, I. M., and Dewey, J., 1990. Statistical analysis of the results of earthquake prediction, based on burst of aftershocks. *Phys. Earth Planet. Int.*, 61, 128–139.
- [99] Knopoff, L., Levshina, T., Keilis-Borok, V. I., and Mattoni, C., 1996. Increased long-range intermediate-magnitude earthquake activity prior to strong earthquakes in California. *J. Geophys. Res.*, 101, 5779–5796.
- [100] Bufe, C. G. and Varnes, D. J., 1993. Predictive modeling of the seismic cycle of the Greater San Francisco Bay region. *J. Geophys. Res.*, 98, 9871–9883.
- [101] Bowman, D. D., Ouillon, G., Sammis, C. G., Somette, A., and Sornette, D., 1998. An observational test of the critical earthquake concept, *J. Geophys. Res.*, 103, 24359–24372.
- [102] Richtmyer, R.D., and Morton, K.W., 1967. *Difference Methods for Initial-Value Problems*, Wiley, New York (2nd ed), 420pp.
- [103] Wolfram, S., 1983. Statistical-mechanics of cellular automata. *Rev. Modern Phys.*, 55 (3), 601–644.

- [104] Wolfram, S., 1984. Universality and complexity in cellular automata. *Physica D*, 10 (1-2), 1–7.
- [105] Wright, D. G., Stocker, T. F., and Mysak, L. A., 1990, A note on Quaternary climate modelling using Boolean delay equations. *Climate Dyn.*, 4, 263–267.
- [106] Nicolis, C., 1982. Boolean approach to climate dynamics. *Q. J. R. Meteorol. Soc.*, 108, 707–715.
- [107] Mysak, L. A., D. K. Manak, and R. F. Marsden, 1990. Sea-ice anomalies observed in the Greenland and Labrador Seas during 1901–1984 and their relation to an interdecadal Arctic climate cycle. *Climate Dyn.*, 5, 111–113.
- [108] Kellogg, W. W., 1983. Feedback mechanisms in the climate system affecting future levels of carbon dioxide. *J. Geophys. Res.*, 88, 1263–1269.
- [109] Neumann, A. and Weisbuch, G., 1992. Window automata analysis of population dynamics in the immune system. *Bull. Math. Biol.* 54, 21–44.
- [110] Neumann, A. and Weisbuch, G., 1992. Dynamics and topology of idiotypic networks. *Bull. Math. Biol.* 54, 699–726.

Table 1. Common Boolean operators

Mathematical symbol	Engineering symbol	Name	Comment
\bar{x}	NOT x	negator	not true when x is true
$x \vee y$	x OR y	logical or	true when either x or y or both are true
$x \wedge y$	x AND y	logical and	$x \wedge y \equiv \overline{(\bar{x} \vee \bar{y})}$
$x \nabla y$	x XOR y	exclusive or	not true when x and y are equal
$x \triangle y$			true when x and y are equal

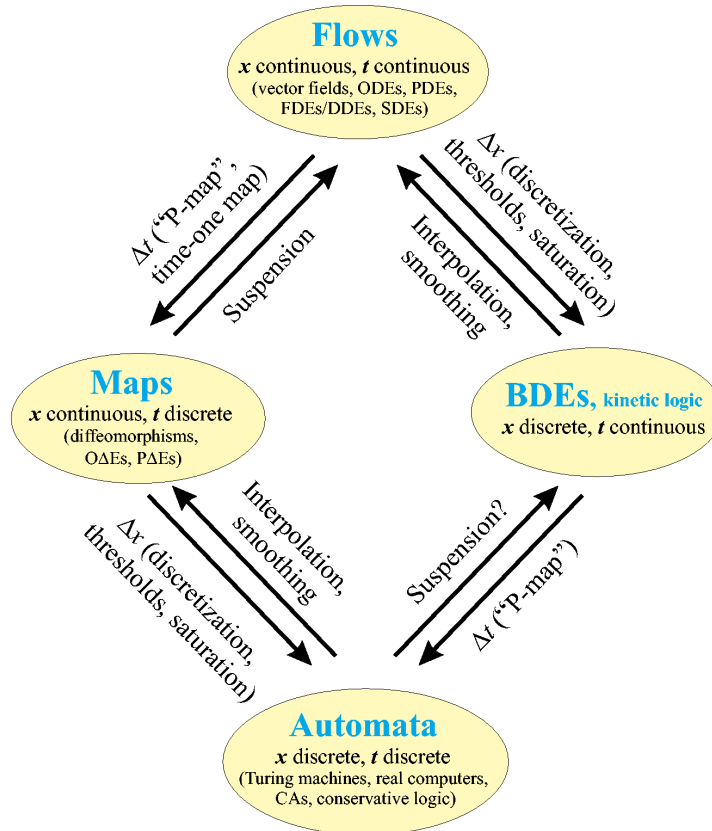


Figure 1: The place of BDEs within dynamical system theory. Note the links: The discretization of t can be achieved by the Poincaré map (P-map) or a time-one map, leading from **Flows** to **Maps**. The opposite connection is achieved by suspension. To go from **Maps** to **Automata** we use the discretization of x . Interpolation and smoothing can lead in the opposite direction. Similar connections lead from **BDEs** to **Automata** and to **Flows**, respectively. Modified after Mullhaupt [2].

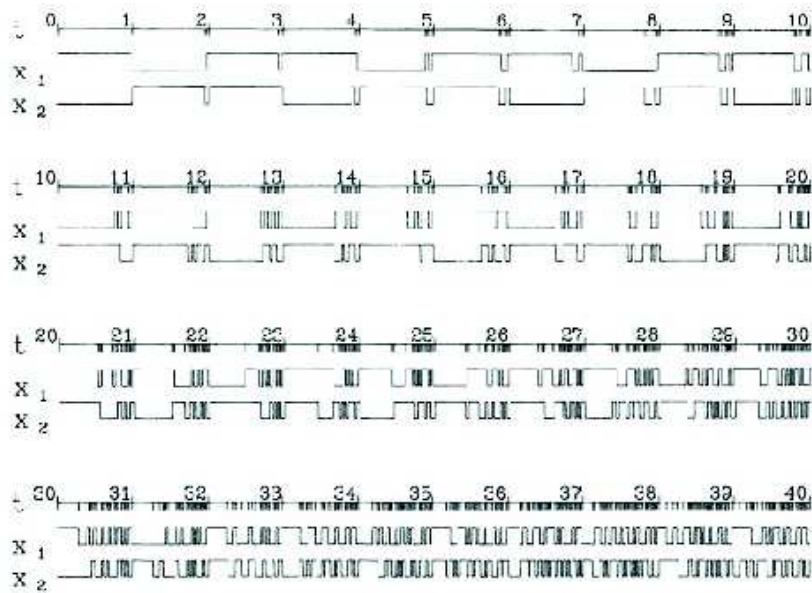


Figure 2: Solutions of the system of BDEs $x_1(t) = x_2(t - \theta)$, $x_2(t) = x_1(t - \theta) \nabla x_2(t - 1)$ for $\theta = 0.977$ and $0 \leq t < 40$ [1]. The symbol ∇ stands for the ‘exclusive or’ (see Table 1). The tick marks on the t -axis indicate the times at which jumps in either x_1 or x_2 take place. After Dee and Ghil [1]. Copyright ©Society for Industrial and Applied Mathematics; reprinted with permission.

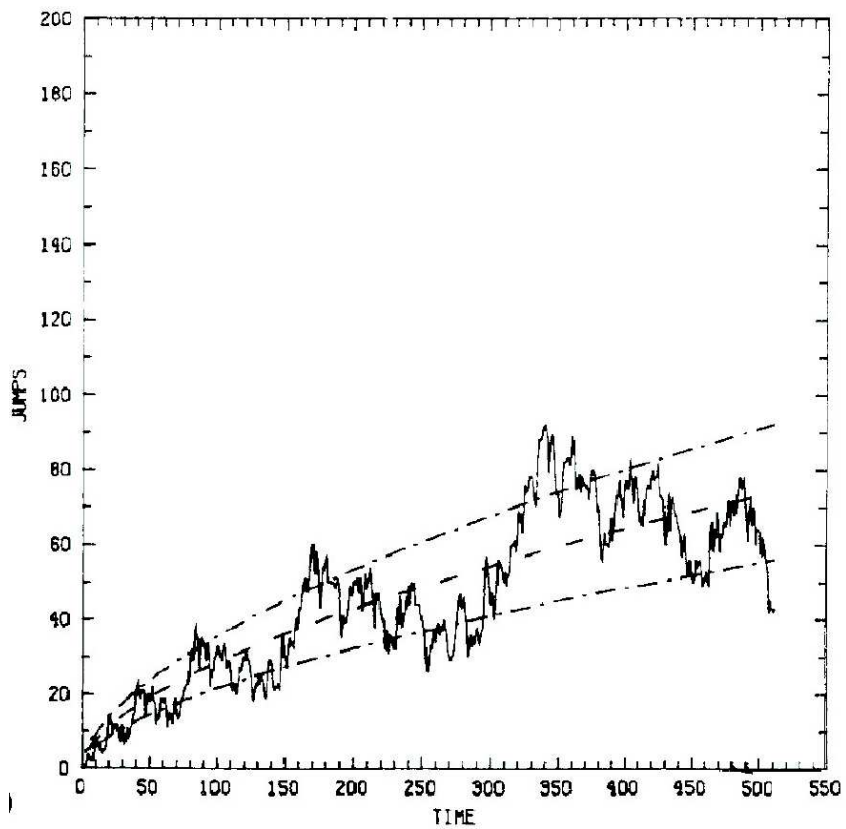


Figure 3: Jump function $J(t)$ for the particular solution of Eq. (8) described in the text. Reproduced from [3], with kind permission of Springer Science and Business Media.

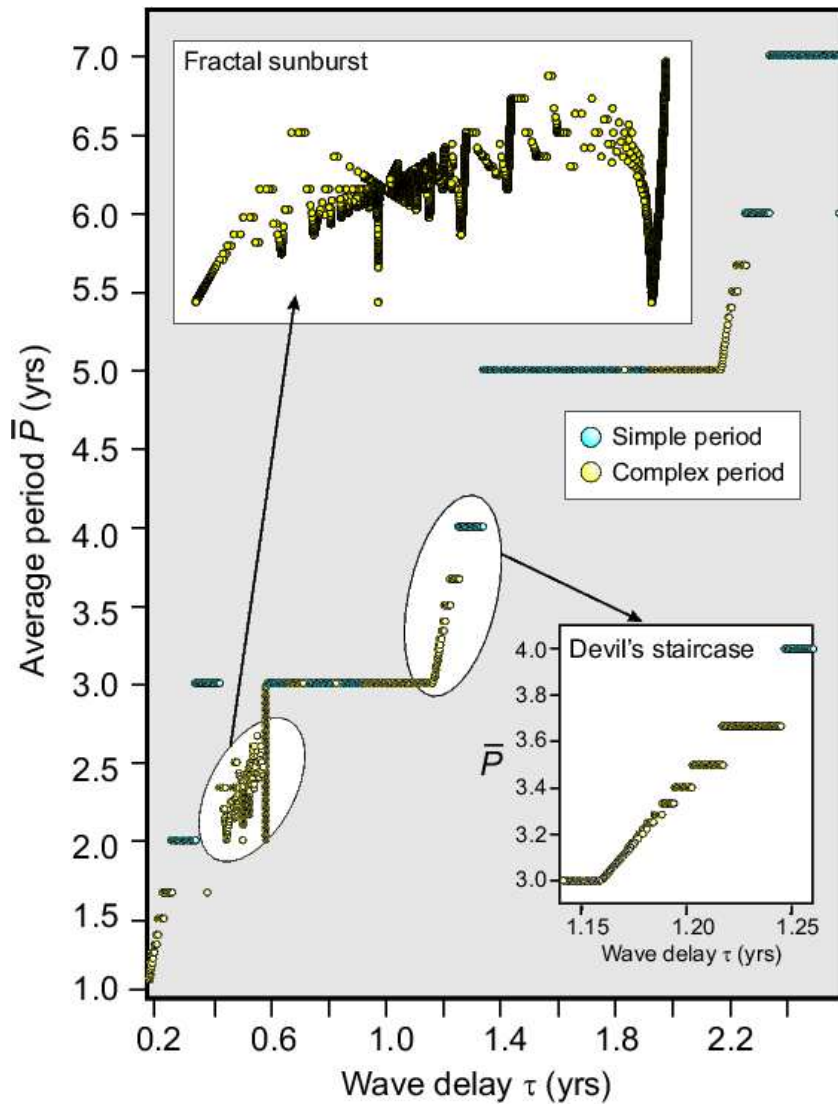


Figure 4: Devil’s staircase and fractal sunburst: A bifurcation diagram showing the average cycle length \bar{P} vs. the wave delay τ for a fixed $\beta = 0.17$. Blue dots indicate purely periodic solutions; orange dots are for complex periodic solutions; small black dots denote aperiodic solutions. The two insets show a blow-up of the overall, approximate Devil’s staircase between periodicities of two and three years (“fractal sunburst”) and of three and four years (“Devil’s staircase”). Modified after Saunders and Ghil [7].

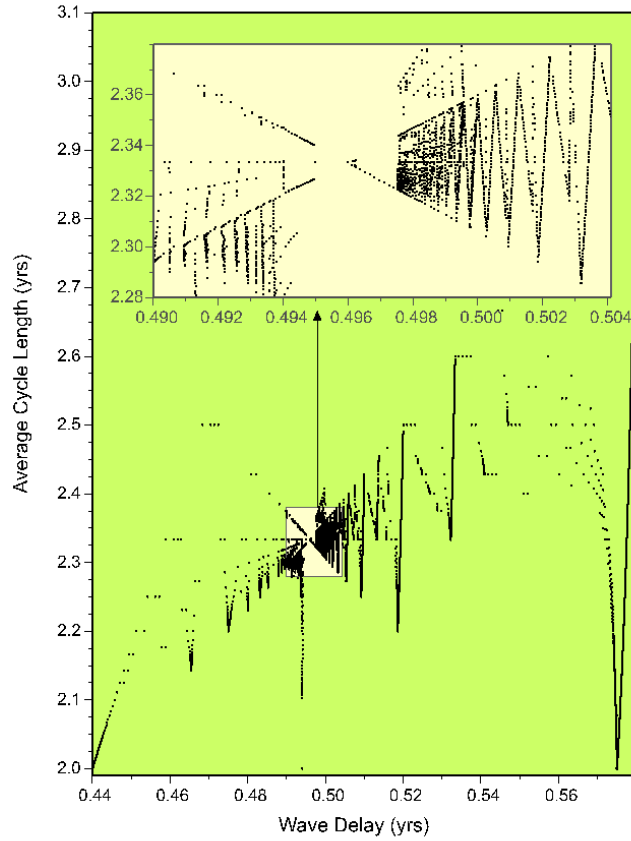


Figure 5: Fractal sunburst: a BDE solution pattern in phase-parameter space. A blow-up of the transition zone from average periodicity two to three years; $\tau = 0.4\text{--}0.58, \beta = 0.17$. The inset is a zoom on $0.49 \leq \tau \leq 0.504$. A complex mini-staircase structure reveals self-similar features, with a focal point at $\tau \approx 0.5$. Modified after Saunders and Ghil [7].

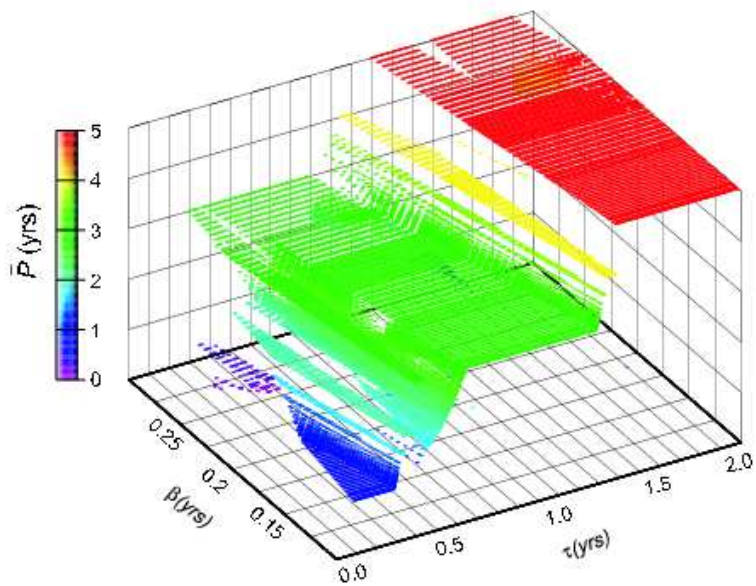


Figure 6: The Devil’s bleachers: A three-dimensional regime diagram showing the average cycle length \bar{P} , portrayed in both height and color, vs. the two delays β and τ . Oscillations are produced even for very small values of β , as long as $\beta \leq \tau$. Variations in τ determine the oscillation’s period, while changing β establishes the bottom step of the staircase, shifts the location of the steps, and determines their width. After Saunders and Ghil [7].

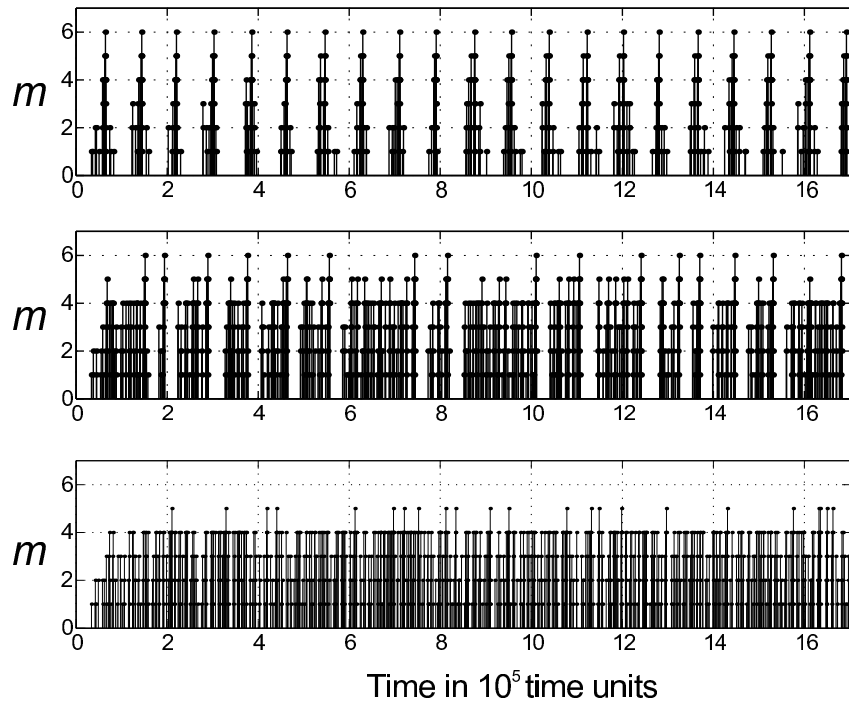


Figure 7: Three seismic regimes: sample of earthquake sequences. Top panel – regime **H** (High), $\Delta_H = 0.5 \cdot 10^4$; middle panel – regime **I** (Intermittent), $\Delta_H = 10^3$; bottom panel – regime **L** (Low), $\Delta_H = 0.5 \cdot 10^3$. Only a small fraction of each sequence is shown, to illustrate the differences between regimes. Reproduced from Zaliapin *et al.* [8], with kind permission of Springer Science and Business Media.

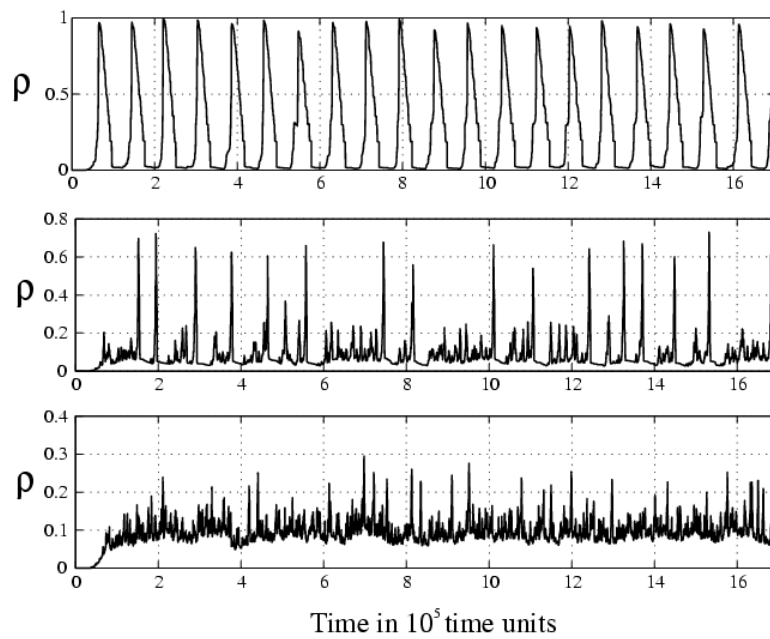


Figure 8: Three seismic regimes: internal dynamics of the system. The panels show the density $\rho(n)$ of broken elements in the system, as defined by Eq.(20); they correspond to the synthetic sequences shown in Fig. 7. Top panel – Regime **H**; middle panel – Regime **I**; and bottom panel – regime **L**. Reproduced from Zaliapin *et al.* [8], with kind permission of Springer Science and Business Media.

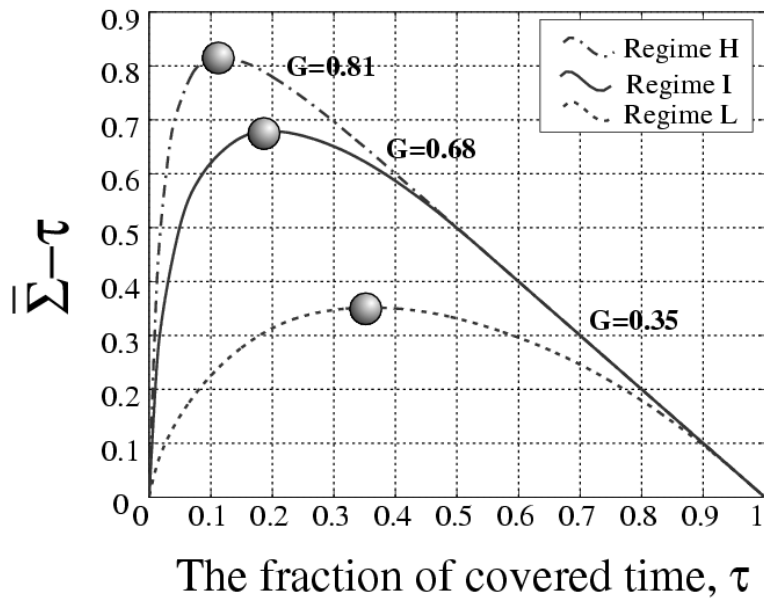


Figure 9: Measure $\mathcal{G}(I)$ of seismic clustering; see Eq. (25). The three curves correspond to the three synthetic sequences shown in Fig. 7. Reproduced from Zaliapin *et al.* [8], with kind permission of Springer Science and Business Media.

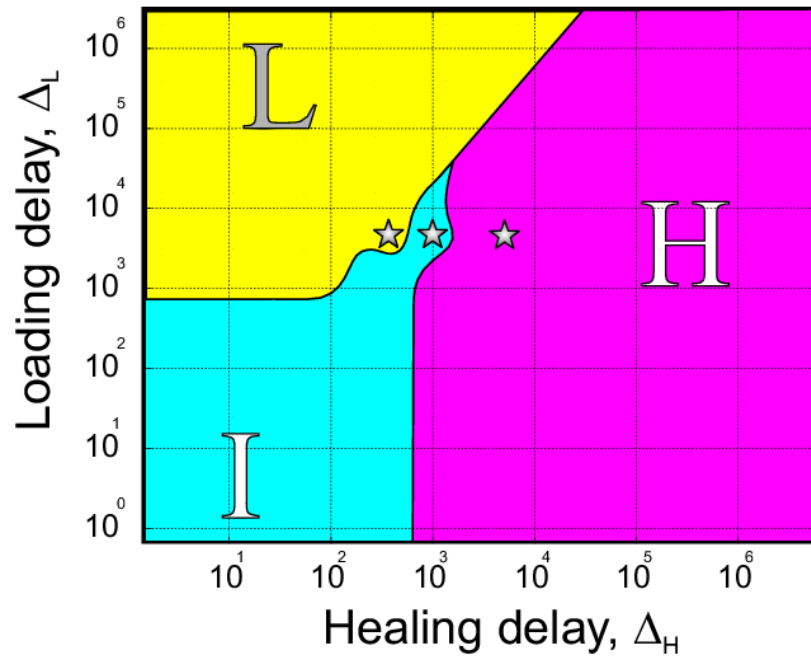


Figure 10: Regime diagram in the (Δ_L, Δ_H) plane of the loading and healing delays. Stars correspond to the sequences shown in Fig. 7. Reproduced from Zaliapin *et al.* [8], with kind permission of Springer Science and Business Media.

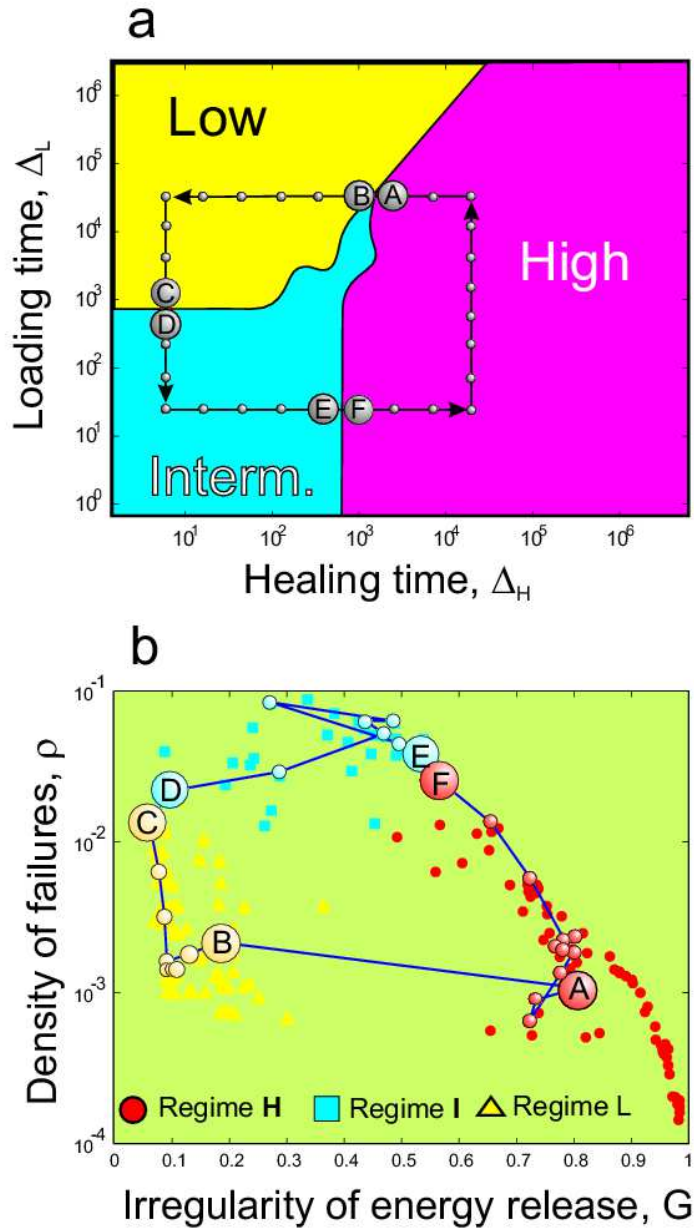


Figure 11: Bifurcation diagram for the BDE seismic model. a) Rectangular path in the delay plane (Δ_L , Δ_H); b) The measures \mathcal{G} and ρ , calculated along the rectangular path shown in panel (a). The transition between points (A) and (B), *i.e.* between regimes **H** and **L**, is very sharp with respect to the change in irregularity \mathcal{G} of energy release, while almost negligible with respect to the change in failure density ρ . The colored circles, triangles, and squares in panel b) correspond to synthetic catalogs from regimes **H**, **I**, and **L** respectively; these catalogs do not belong to the rectangular path in panel a).

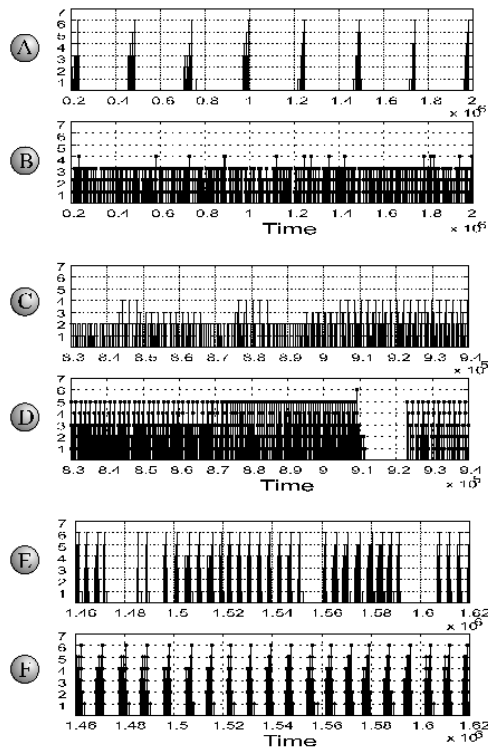


Figure 12: Synthetic sequences corresponding to the points along the path in parameter space (Fig. 11a). The panels illustrate the transitions between the regimes **H** and **L** — panels (A) and (B); **L** and **I** — (C) and (D); and **I** and **H** — (E) and (F). The transition from (A) to (B) is very pronounced, while the other two transitions are smoother. Reproduced from Zaliapin *et al.* [8], with kind permission of Springer Science and Business Media.

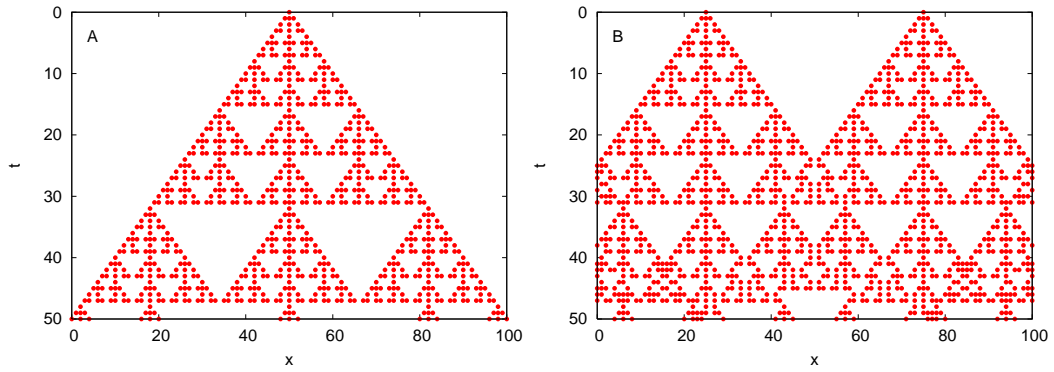


Figure 13: Solutions of the “partial BDE” (29): (a) for a single nonzero site at $t = 0$; and (b) the collision of two “waves,” each originating from such a site. For the space and time steps $h = k = 1$, this BDE is equivalent to the elementary cellular automaton (ECA) with rule 150.

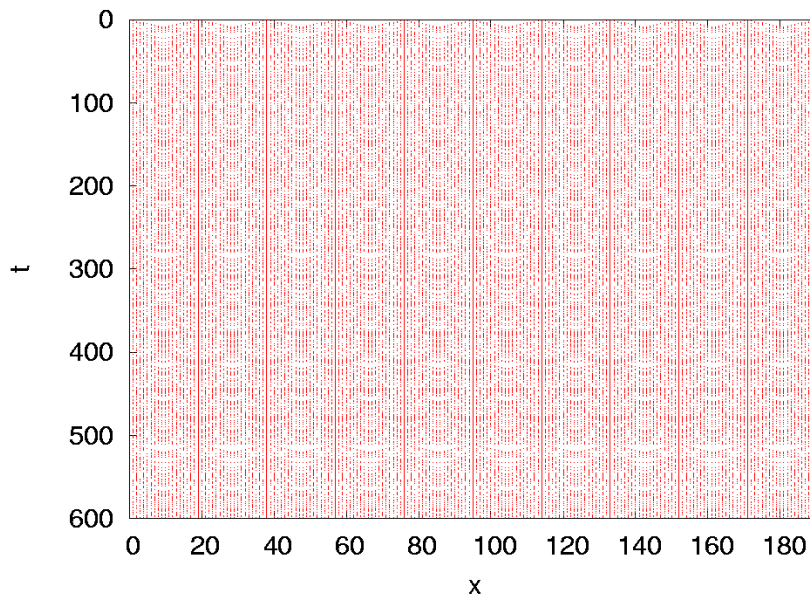


Figure 14: The solution of the BDE (29) from a periodic initial state of spatial period $T_x = 19$. The solution asymptotes rapidly to a very long temporal period of $T_t = 511$.

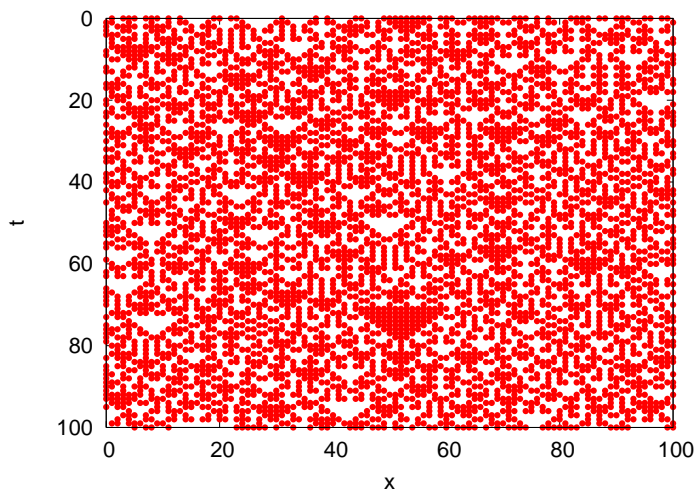


Figure 15: The solution of the BDE (29) starting from a random initial state of length $N = 100$. The qualitative behavior is characterized by “triangles” of empty or occupied sites but without any recurrent pattern, and it does not depend on the particular random initial state.